Table 2
Scores of antisocial behavior

Behavior	Scores of antisocial behavior	n
	Mean (SD; range)	
Stealing	6.38 (3.42; 0–12)	8/22
Traffic accident	3.46 (3.46; 0–12)	4/22
Physical assault	4.50 (4.34; 0–12)	8/22
Sexual comments/advances	7.67 (2.31; 0–9)	3/22
Public urination	3.67 (1.86; 0–6)	6/22
Total	9.67 (6.82; 0–25)	18/22

n = number of subjects who showed the behavior. n for total means of subjects who showed at least one of the behavior.

room. Ten minutes after injection, brain SPECT was performed using a triple-headed gamma camera (MULTISPECT 3; Siemens, Hoffman Estates, IL) equipped with high-resolution fanbeam collimators. For each scan, projection data were obtained in 128 × 128 matrix, and camera was rotated through 120° with 24 steps of 50 s per step. SPECT images were reconstructed using a Shepp and Logan Hanning filter at 0.7 cycles per centimeter. Attenuation correction was performed using Chang's method.

Image analysis

Voxel-based analysis of SPECT data was performed using Statistical Parametric Mapping 99 (SPM99) (Wellcome Department of Cognitive Neurology, London, U.K.) run on MATLAB (The MathWorks, Inc., Sherborn, MA). The images were spatially normalized to an original template for ^{99m}Tc-ECD using SPM99 (Ohnishi et al., 2000). Images were then smoothed with a gaussian kernel of 12 mm in full width half maximum (FWHM). The washout correction for ^{99m}Tc-ECD was not applied, because brain SPECT was started at 10 min after injection.

Statistical analysis of SPECT data

The processed images were analyzed using SPM99 as described by Ohnishi et al. (2000). The effect of global differences in CBF among scans was removed by proportional scaling with the gray matter threshold at 0.5. The subject and the covariate effects were estimated with a general linear model at each voxel. To test hypotheses about regional population effects, the estimates were compared using linear compounds or contrasts. The resulting sets of t values constituted statistical parametric maps (SPM$\{t\}$). The SPM$\{t\}$ were transformed to unit normal distribution (SPM$\{Z\}$) and thresholded at $P < 0.005$. To correct for the multiple non-independent comparisons that were inherent in this analysis, the resulting foci were characterized for their spatial extent. This characterization, regarding probability, is to assess whether the region of the observed number of voxels could have occurred by chance over the entire volume analyzed.

Correlation analysis was performed to study the relationship between rCBF changes and antisocial behavioral profiles. The correlations between the scores of antisocial behaviors and CBF, MMSE scores and CBF, and the duration of illness and CBF were respectively computed on a pixel-by-pixel basis by covariance analysis. Gender and age were treated as nuisance variables.

Statistical analysis of antisocial behavioral symptoms

Statistical data analysis of antisocial behavioral symptoms in FTD patients was performed using the R software (The R Foundation for Statistical Computing, Vienna, Austria).

Results

Antisocial behavioral symptoms in FTD patients

Eighteen of the 22 FTD patients had a history of antisocial behavior. The mean score of the antisocial behavior was 9.67 ± 6.82 (range, 0–25). The mean value of Cohen's κ coefficient of all the items for inter-rater was 0.82 (range, 0.67–0.91), which appears to be satisfactory. Table 2 shows the subscale score of the 5 antisocial behaviors of the patients.

Changes in rCBF in FTD patients

Decreases of rCBF in the FTD patients compared with the normal healthy volunteers were identified in the superior, the middle, and the inferior frontal gyrus. In addition, there were reductions of rCBF in the subcortical structures, particularly the caudate nuclei and the thalami (Fig. 1).

As a result of the correlation analysis, a positive correlation was observed between the scores of antisocial behavioral symptoms

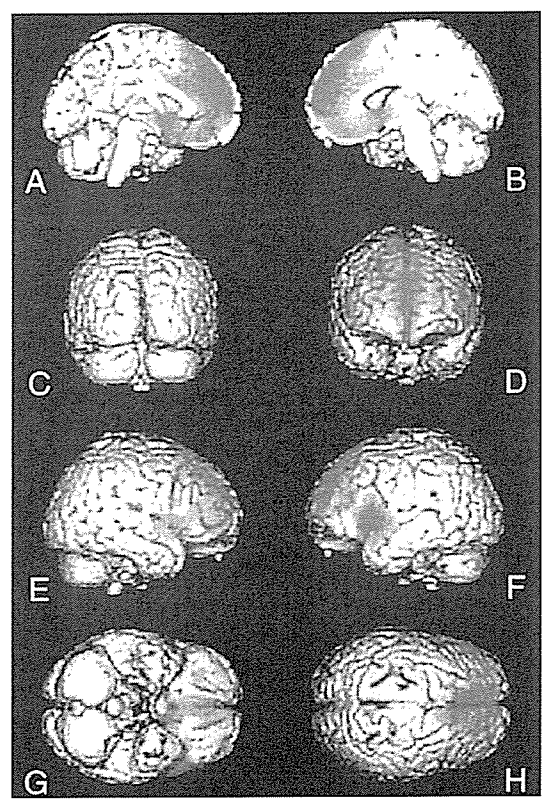

Fig. 1. Result of SPM analysis (normal healthy volunteers vs. FTD patients). The colored areas show the regions with lower perfusion in the FTD patients compared with the normal healthy volunteers ($P < 0.005$, uncorrected for multiple comparisons). View from medial right (A), medial left (B), posterior (C), anterior (D), right lateral (E), left lateral (F), inferior (G), and superior (H). Rt = right, Lt = left.

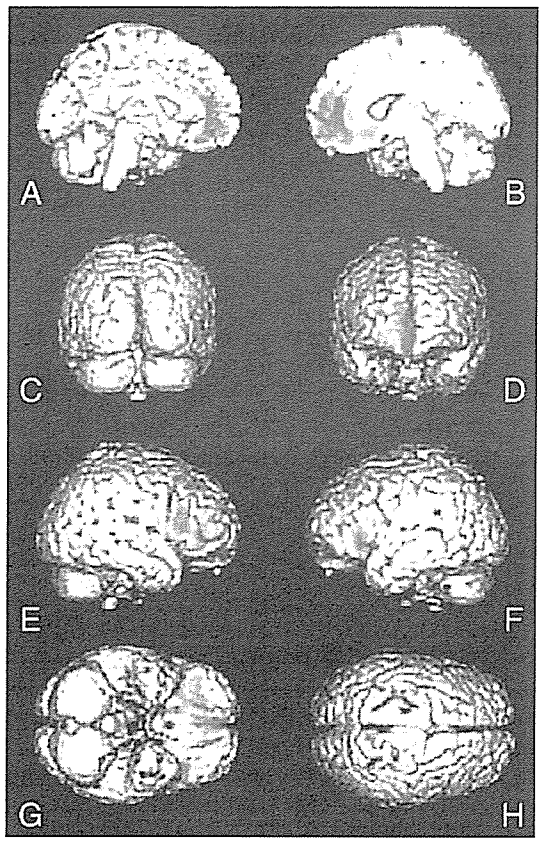

Fig. 2. Result of SPM analysis: the areas of regional cerebral blood flow that correlated with the score of antisocial behaviors in patients with FTD. Representation in stereotaxic space of cerebral regions that correlated positively with the score of antisocial behaviors ($P < 0.005$, uncorrected for multiple comparisons), displayed on 3D-surface anatomical template. View from medial right (A), medial left (B), posterior (C), anterior (D), right lateral (E), left lateral (F), inferior (G), and superior (H). Rt = right, Lt = left.

and the rCBF in partial areas of the orbitofrontal cortex (Fig. 2): the bilateral inferior frontal gyri (Broadmann area, BA 47), the left anterior cingulated gyrus (BA 32), the right caudate nucleus, and the left insula (BA 13). The results were similar even when the scores were independently analyzed for the severity scores and the frequency scores. We searched for a negative correlation between rCBF and the scores of antisocial behavioral symptoms, but no significant finding was found in any of the regions.

On the other hand, the MMSE scores positively correlated with rCBF in the bilateral posterior cingulate gyri (BA 31), the right parahippocampal gyrus (BA 30), and the right insula (BA 13) (Fig. 3). Furthermore, a correlation between the duration of illness and rCBF was observed in the right middle frontal gyrus (BA 47) and the bilateral inferior frontal gyri (BA 46, 47), as well as the left superior temporal gyrus (BA 22), the middle temporal gyrus (BA 21), and the parahippocampal gyrus (BA 27) (Fig. 4). The two analyses have resulted to have BA 47, which constitutes the orbitofrontal cortex, in common.

Discussion

FTD is the third most common neurodegenerative dementia syndrome after Alzheimer's disease and dementia with Lewy bodies. Although criteria for clinical diagnosis of FTD, such as the Lund and Manchester criteria and the more recent consensus criteria (Neary et al., 1998), have high sensitivities and specificities for diagnosing FTD (Lopez et al., 1999), clinicians frequently fail to recognize FTD or misdiagnose it as Alzheimer's disease, manic-depressive illness, schizophrenia, depression, hypochondriasis, obsessive–compulsive disorder, or sociopathy (Litvan et al., 1997; McKhann et al., 2001). The core diagnostic features of FTD are early loss of personal and social awareness, early loss of insight, early decline in social interpersonal conduct, impaired regulation of personal conduct, and emotional blunting. Thus, the most common and early symptom of FTD can be summarized as a decline in social interpersonal conduct (Neary et al., 1998).

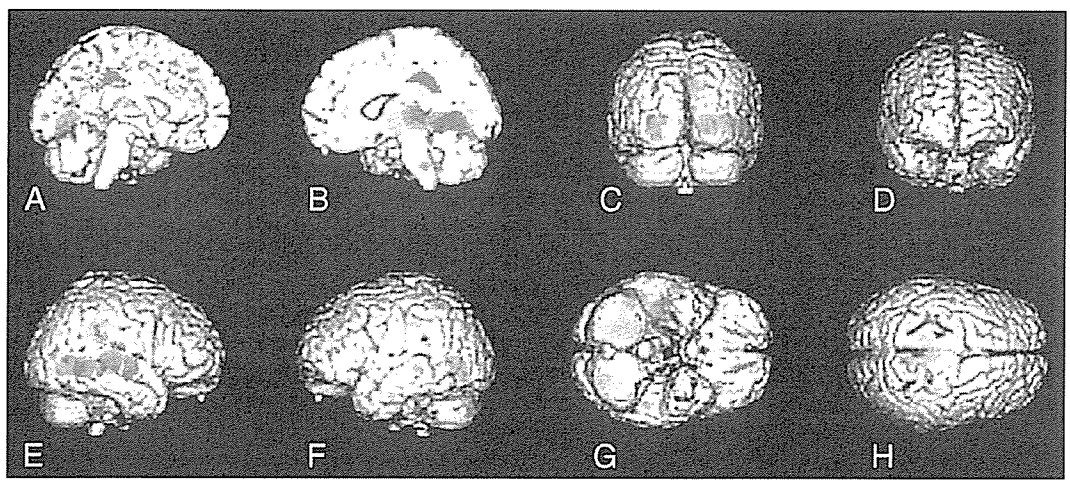

Fig. 3. Result of SPM analysis: the areas of regional cerebral blood flow that correlated with the score of MMSE in patients with FTD. Representation in stereotaxic space of cerebral regions that correlated positively with the score of MMSE ($P < 0.005$, uncorrected for multiple comparisons), displayed on 3D-surface anatomical template. View from medial right (A), medial left (B), posterior (C), anterior (D), right lateral (E), left lateral (F), inferior (G), and superior (H). Rt = right, Lt = left.

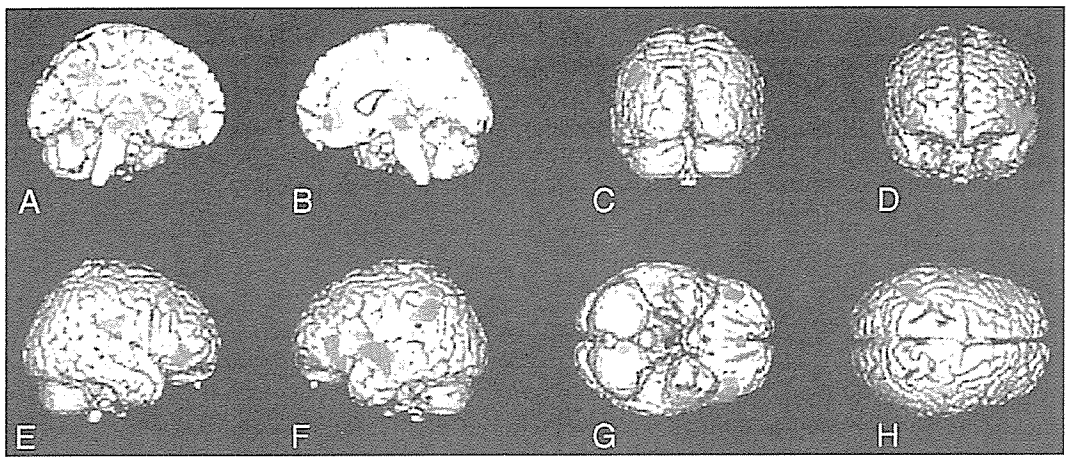

Fig. 4. Result of SPM analysis: the areas of regional cerebral blood flow that correlated with the duration of illness in patients with FTD. Representation in stereotaxic space of cerebral regions that correlated positively with the score of the duration of illness ($P < 0.005$, uncorrected for multiple comparisons), displayed on 3D-surface anatomical template. View from medial right (A), medial left (B), posterior (C), anterior (D), right lateral (E), left lateral (F), inferior (G), and superior (H). Rt = right, Lt = left.

Antisocial behavior, from Pick's case report (Pick, 1892), has been reported in association with FTD for decades (Gustafson, 1987; Lindau et al., 2000; Hokoishi et al., 2001; Hodges, 2001). They include stealing, traffic accident, physical assault, sexual comments/advances, public urination, and so on. In fact, 18 of 22 (82%) FTD patients of the present study showed such behaviors. This figure is similar with the results reported in the previous studies (Miller et al., 1997).

Although a variety of scales to rate the Behavioral and Psychological Symptoms of Dementia (BPSD) observed in patients with AD is reported, to our knowledge, no scale is available for the assessment of BPSD observed in FTD patients. Thus, we employed the assessment method of the Neuropsychiatric Inventory (NPI) (Cummings et al., 1994) for AD patients. The NPI assesses BPSD on the basis of both frequency and severity. The focused symptoms are derived from the report by Miller et al. on BPSD of FTD patients.

In the comparison between the FTD patients and the normal healthy volunteers, a significant reduction of rCBF in the widespread frontal lobes was observed in the former. No other region with significantly decreased rCBF was found. The results seem to be compatible with the neuropathological and functional changes of the disease and are consistent with the findings of previous FDG-PET studies (Ishii et al., 1998; Salmon et al., 2003; Grimmer et al., 2004). Although the diagnosis of the present study was not confirmed by postmortem examination, the result appears to support the validity of our diagnosis of FTD, the frontal variants of FTLD.

Regarding the frontal lobe function, it is well known that prefrontal cortex dysfunction is linked to social misconduct (Harlow, 1868; Eslinger, 1999; Bassarath, 2001; Brower and Price, 2001). Stuss and Benson (1986) have noted that orbitofrontal pathology would most frequently be associated with disinhibition, facetiousness, sexual and personal hedonism, and lack of concern for others. Moreover, a recent PET study evaluating patients with various frontal lobe pathologies (including FTD) (Sarazin et al., 1998) with ROI approach has revealed that the behavioral abnormalities are associated with metabolic decline of orbitofrontal cortex. Also, it is now well known that prefrontal cortex plays a major role in executive function and working memory (Lezak, 1983). Anterior cingulate gyrus and cortex are associated with sustained attention (Posner and Petersen, 1990). Although dysfunction of the orbitofrontal cortex plays a major role, failure of these cognitive functions may be functionally involved together and contribute to the development of the antisocial behaviors.

The highlight of our voxel-by-voxel SPECT study using the SPM technique is the finding that the decrement of orbitofrontal rCBF is associated with antisocial behaviors as well as the duration of illness in the patients with FTD. MMSE score, on the contrary, did not correlate with rCBF of the orbitofrontal cortex. A recent longitudinal study in FTD has shown that the metabolic activity in the orbitofrontal cortex decreases as the disease progresses (Grimmer et al., 2004). In this multicenter study, the conjunction analysis using SPM has demonstrated that the metabolic impairment of orbitofrontal cortex is affected in every FTD patients (Grimmer et al., 2004). Although this study did not examine the association between metabolic impairment of orbitofrontal cortex and antisocial behaviors, it may support the results of the present study to some extent. Taking these findings together, the association between antisocial behaviors and rCBF of orbitofrontal cortex in FTD may appear to be robust.

We must refer to several limitations of the present study. As described above, we did not pathologically confirm the clinical diagnosis. However, clinical criteria of FTD are reported to have high specificities (Rosen et al., 2002). SPM analysis for SPECT study also has limitations; it can be affected by partial volume effect (PVE). Matsuda et al. (2002) have established a PVE correction method for SPECT study and reported its utility. In this study, however, we did not correct the PVE. In future study, correlation analysis between antisocial behavior and rCBF using PVE correction is necessary. We also attempted to clarify the relationship between the duration of illness and rCBF, but since the onset of FTD is insidious and its progression is gradual, the duration of illness remained uncertain (Neary et al., 1998). Moreover, the number of the subjects was relatively small. Future studies should overcome these limitations.

In summary, the orbitofrontal dysfunction appears to play a major role in the emergence of antisocial behaviors in FTD patients.

References

Anne, T., Stephan, F., 1969. The Stroop test: selective attention to colours and words. Nature 222, 437–439.

Bassarath, L., 2001. Neuroimaging studies of antisocial behaviour. Can. J. Psychiatry 46, 728–732.

Brower, M.C., Price, B.H., 2001. Neuropsychiatry of frontal lobe dysfunction in violent and criminal behaviour: a critical review. J. Neurol. Neurosurg. Psychiatry 71, 720–726.

Charpentier, P., Lavenu, I., Defebvre, L., Duhamel, A., Lecouffe, P., Pasquier, F., Steinling, M., 2000. Alzheimer's disease and frontotemporal dementia are differentiated by discriminant analysis applied to (99m)Tc HmPAO SPECT data. J. Neurol. Neurosurg. Psychiatry 69, 661–663.

Cummings, J.L., Mega, M., Gray, K., Rosenberg-Thompson, S., Carusi, D.A., Gornbein, J., 1994. The neuropsychiatric inventory: comprehensive assessment of psychopathology in dementia. Neurology 44, 2308–2314.

Eslinger, P.J., 1999. Orbital frontal cortex: historical and contemporary views about its behavioral and physiological significance. An introduction to special topic papers: Part I. Neurocase 5, 225–229.

Folstein, M.F., Folstein, S.E., McHugh, P.R., 1975. Mini-mental state. A practical method for grading the cognitive state of patients for the clinician. J. Psychiatr. Res. 12, 189–198.

Frackowiack, R.S.J., Friston, K.J., Frith, C.D., Dolan, R.J., Mazziotta, J.C., 1997. Human Brain Function. Calif: Academic Press, San Diego.

Grimmer, T., Diehl, J., Drzezga, A., Forstl, H., Kurz, A., 2004. Region-specific decline of cerebral glucose metabolism in patients with frontotemporal dementia: a prospective 18F-FDG-PET study. Dement. Geriatr. Cogn. Disord. 18, 32–36.

Gustafson, L., 1987. Frontal lobe degeneration of non-Alzheimer type: II. Clinical picture and differential diagnosis. Arch. Gerontol. Geriatr. 6, 209–223.

Harlow, J., 1868. Recovery from passage of an iron bar through the head. Publications of the Massachusetts Medical Society 2, 329–346.

Hodges, J.R., 1993. Cognitive Assessment for Clinicians, 1st ed. Oxford Medical, Oxford, England, pp. 197–228.

Hodges, J.R., 2001. Frontotemporal dementia (Pick's disease): clinical features and assessment. Neurology 56, S6–S10.

Hokoishi, K., Ikeda, M., Maki, N., Nebu, A., Shigenobu, K., Fukuhara, R., Komori, K., Tanabe, H., 2001. Frontotemporal lobar degeneration: a study in Japan. Dement. Geriatr. Cogn. Disord. 12, 393–399.

Imabayashi, E., Matsuda, H., Asada, T., Ohnishi, T., Sakamoto, S., Nakano, S., Inoue, T., 2004. Superiority of 3-dimensional stereotactic surface projection analysis over visual inspection in discrimination of patients with very early Alzheimer's disease from controls using brain perfusion SPECT. J. Nucl. Med. 45, 1450–1457.

Imai, Y., Hasegawa, K., 1999. In: Burns, A., Lawlor, B., Craig, S. (Eds.), Assessment Scales In Old Age Psychiatry. Martin Dunitz, London, p. 71.

Ishii, K., Sakamoto, S., Sasaki, M., Kitagaki, H., Yamaji, S., Hashimoto, M., Imamura, T., Shimomura, T., Hirono, N., Mori, E., 1998. Cerebral glucose metabolism in patients with frontotemporal dementia. J. Nucl. Med. 39, 1875–1878.

Lezak, M.D., 1983. Neuropsychological Assessment, 2nd ed. Oxford UP, New York.

Lindau, M., Almkvist, O., Kushi, J., Boone, K., Johansson, S.E., Wahlund, L.O., Cummings, J.L., Miller, B.L., 2000. First symptoms-frontotemporal dementia versus Alzheimer's disease. Dement. Geriatr. Cogn. Disord. 11, 286–293.

Litvan, I., Agid, Y., Sastry, N., Jankovic, J., Wenning, G.K., Goetz, C.G., Verny, M., Brandel, J.P., Jellinger, K., Chaudhuri, K.R., McKee, A., Lai, E.C., Pearce, R.K., Bartko, J.J., 1997. What are the obstacles for an accurate clinical diagnosis of Pick's disease? A clinicopathologic study. Neurology 49, 62–69.

Lojkowska, W., Ryglewicz, D., Jedrzejczak, T., Sienkiewicz-Jarosz, H., Minc, S., Jakubowska, T., Kozlowicz-Gudzinska, I., 2002. SPECT as a diagnostic test in the investigation of dementia. J. Neurol. Sci. 15, 215–219.

Lopez, O.L., Litvan, I., Catt, K.E., Stowe, R., Klunk, W., Kaufer, D.I., Becker, J.T., DeKosky, S.T., 1999. Accuracy of four clinical diagnostic criteria for the diagnosis of neurodegenerative dementias. Neurology 53, 1292–1299.

Matsuda, H., Kanetaka, H., Ohnishi, T., Asada, T., Imabayashi, E., Nakano, S., Katoh, A., Tanaka, F., 2002. Brain SPET abnormalities in Alzheimer's disease before and after atrophy correction. Eur. J. Nucl. Med. Mol. Imaging 29 (11), 1502–1505.

McKhann, G.M., Albert, M.S., Grossman, M., Miller, B., Dickson, D., Trojanowski, J.Q., 2001. Work Group on Frontotemporal Dementia and Pick's Disease. Clinical and pathological diagnosis of frontotemporal dementia: report of the work group on frontotemporal dementia and pick's disease. Arch. Neurol. 58, 1803–1809.

Miller, B.L., Gearhart, R., 1999. Neuroimaging in the diagnosis of frontotemporal dementia. Dement. Geriatr. Cogn. Disord. 10, S71–S74.

Miller, B.L., Darby, A., Benson, D.F., Cummings, J.L., Miller, M.H., 1997. Aggressive, socially disruptive and antisocial behaviour associated with fronto-temporal dementia. Br. J. Psychiatry 170, 150–154.

Mychack, P., Kramer, J.H., Boone, K.B., Miller, B.L., 2001. The influence of right frontotemporal dysfunction on social behavior infrontotemporal dementia. Neurology 56, S11–S15.

Neary, D., Snowden, J.S., Gustafson, L., Passant, U., Stuss, D., Black, S., Freedman, M., Kertesz, A., Robert, P.H., Albert, M., Boone, K., Miller, B.L., Cummings, J., Benson, D.F., 1998. Frontotemporal lobar degeneration: a consensus on clinical diagnostic criteria. Neurology 51, 1546–1554.

Ohnishi, T., Matsuda, H., Hashimoto, T., Kunihiro, T., Nishikawa, M., Uema, T., 2000. Abnormal regional cerebral blood flow in childhood autism. Brain 123, 1838–1844.

Pick, A., 1892. Uber die Beziehungen der senilen Hirnatrophie zur Aphasie. Prager Medizinische Wochenschrift 17, 165–167.

Posner, M.I., Petersen, S.E., 1990. The attention system of the human brain. Ann. Rev. Neurosci. 13, 25–42.

Rosen, H.J., Hartikainen, K.M., Jagust, W., Kramer, J.H., Reed, B.R., Cummings, J.L., Boone, K., Ellis, W., Miller, C., Miller, B.L., 2002. Utility of clinical criteria in differentiating frontotemporal lobar degeneration (FTLD) from AD. Neurology 58, 1608–1615.

Salmon, E., Garraux, G., Delbeuck, X., Collette, F., Kalbe, E., Zuendorf, G., Perani, D., Fazio, F., Herholz, K., 2003. Predominant ventromedial frontopolar metabolic impairment in frontotemporal dementia. NeuroImage 20, 435–440.

Sarazin, M., Pillon, B., Giannakopoulos, P., Rancurel, G., Samson, Y., Dubois, B., 1998. Clinicometabolic dissociation of cognitive functions and social behavior in frontal lobe lesions. Neurology 51, 142–148.

Stuss, D.T., Benson, D.F., 1986. The Frontal Lobes. Raven Press, New York.

ELSEVIER

NeuroImage

www.elsevier.com/locate/ynimg
NeuroImage 31 (2006) 1445 - 1452

Age-related degeneration of corpus callosum measured with diffusion tensor imaging

Miho Ota,[a,b] Takayuki Obata,[a,c,*] Yoshihide Akine,[a,c] Hiroshi Ito,[a] Hiroo Ikehira,[c] Takashi Asada,[d] and Tetsuya Suhara[a]

[a]*Department of Molecular Neuroimaging, Molecular Imaging Center, National Institute of Radiological Sciences, 4-9-1 Anagawa, Inage-ku, Chiba 263-8555, Japan*
[b]*Comprehensive Human Sciences, Medical Sciences for Control of Pathological Processes, Clinical Neuroscience, University of Tsukuba Graduate School, Tsukuba, Japan*
[c]*Department of Biophysics, Molecular Imaging Center, National Institute of Radiological Sciences, 4-9-1 Anagawa, Inage-ku, Chiba 263-8555, Japan*
[d]*Department of Psychiatry, University of Tsukuba, Tsukuba, Japan*

Received 12 December 2005; revised 1 February 2006; accepted 3 February 2006
Available online 24 March 2006

The corpus callosum is the major commissure connecting the cerebral hemispheres, and there is evidence of its change with aging. The sub-regions of the corpus callosum (genu, rostral body, anterior midbody, posterior midbody, isthmus, splenium) respectively comprise fibers connecting heteromodal- and unimodal-associated cortical regions, and it is known that abnormalities of the corpus callosum are correlated with abnormalities in cognition and behavior. Yet, little is known about changes in the tissue characteristics of its sub-regions. We assessed age-related changes in fractional anisotropy and mean diffusivity in the sub-regions of the corpus callosum using diffusion tensor imaging. We studied 42 healthy right-handed individuals aged 21–73 years. There were no significant interactions of sex × region. Age has significant negative correlation with fractional anisotropy in the genu ($P < 0.001$), rostral body ($P < 0.001$), and isthmus ($P = 0.005$). Fractional anisotropy of the anterior midbody was correlated negatively with age at a trend level ($P = 0.022$). Age was significantly positively correlated with mean diffusivity in the genu ($P = 0.001$), rostral body ($P = 0.002$), anterior midbody ($P = 0.001$), and isthmus ($P = 0.001$). Age-related changes were detected in the sub-regions where their projection areas are thought to be vulnerable to normal aging. This suggested that fractional anisotropy and mean diffusivity values of the corpus callosum sub-regions could serve as markers of disturbance across the respective projection areas.

Keywords: Corpus callosum sub-region; Diffusion tensor imaging; Fiber tract; Projection area

* Corresponding author. Department of Biophysics, Molecular Imaging Center, National Institute of Radiological Sciences, 4-9-1 Anagawa, Inage-ku, Chiba 263-8555, Japan. Fax: +81 43 253 0396.
E-mail address: t_obata@nirs.go.jp (T. Obata).
Available online on ScienceDirect (www.sciencedirect.com).

1053-8119/$ - see front matter © 2006 Elsevier Inc. All rights reserved.
doi:10.1016/j.neuroimage.2006.02.008

Introduction

The corpus callosum is the major white matter tract that crosses the interhemispheric fissure in the human brain. It consists of approximately 200 million interhemispheric fibers, most of which connect homologous regions of the cerebral cortex (Biegon et al., 1994). The corpus callosum plays an integral role in relaying sensory, motor, and cognitive information between homologous regions in the two cerebral hemispheres (Mazziotta et al., 2001). The corpus callosum is heterogeneous in its microstructural composition (Aboitiz et al., 1992), heterotopic in its anteroposterior cortical connectivity (de Lacoste et al., 1985; Seltzer and Pandya, 1986; Schwartz and Goldman-Rakic, 1991), and differentially susceptible to aging (Aboitiz et al., 1996). Furthermore, specific regions of the corpus callosum (i.e., genu, rostral body, anterior midbody, posterior midbody, isthmus, splenium) are respectively comprised of fibers connecting heteromodally and unimodally associated cortical regions (Huang et al., 2005; Witelson, 1989), and the corpus callosum sub-regions are assumed to have individually different roles of cognition (Baird et al., 2005; Colvin et al., 2005; Madden et al., 2004) that were revealed by the use of diffusion tensor imaging (DTI). Since the corpus callosum sub-regions have their respective original characteristics, the age-related changes they undergo are of particular interest.

Using magnetic resonance imaging (MRI), the morphology of the corpus callosum has been extensively studied. Such studies have shown that abnormalities of the corpus callosum are correlated with abnormalities in cognition (Duara et al., 1991) and behavior (Yazgan and Kinsbourne, 2003) and that callosal features becoming modified during aging indicates modest thinning of its cross-sectional area, measured on midsagittal sections, through young to middle adulthood (Pfefferbaum et al., 1996) with accelerated thinning in older age (Driesen and Raz, 1995; Salat et al., 1997). The gross morphology of the corpus callosum revealed on

conventional MRI, however, does not necessarily reflect the underlying quality of tissue in its microstructure, which is measurable with DTI (Le Bihan, 1995, 2003). DTI allows white matter tracts to be imaged in vivo (Basser and Pierpaoli, 1996) and provides measures of both diffusivity (a measure of mean diffusivity (MD), averaged in all spatial directions) and fractional anisotropy (FA), a measure of the directionality of diffusion (Pierpaoli and Basser, 1996). Degeneration of white matter tracts would be expected to result in a reduction in FA, owing to a loss of directionality of diffusion as a result of the loss of myelin and axonal membranes and possibly due to Wallerian degeneration (Kantarci et al., 2001). With the use of fiber orientation information, one can identify various axonal tracts within the homogeneous-looking white matter. White matter fibers in the brain are essential for linking functional regions. This capability of DTI may be useful for studying the effects of development, aging, and diseases on specific white matter tracts of interest.

There have been several reports on the topic of DTI and aging, and some studies have examined the change of FA in the corpus callosum (Abe et al., 2000; Pfefferbaum et al., 2000; Salat et al., 2005; Sullivan et al., 2001; Hasan et al., 2004; Bhagat and Beaulieu, 2004; Nusbaum et al., 2001; Chepuri et al., 2002). Yet, little is known about changes in the tissue characteristics of the corpus callosum sub-regions. In this study, we investigated the age-related changes of FA and MD in the corpus callosum sub-regions. A full characterization of the patterns of the corpus callosum sub-region microstructure deterioration occurring in normal aging would lead to an understanding of the pathophysiology of normal cognitive decline and would provide a proper background for interpreting the observed changes in neurodegenerative diseases of the aged beyond those of normal aging.

Methods and materials

Subjects

Forty-two healthy individuals (32 men, 10 women; mean age: men 47.3 ± 19.5 years, 21 to 72 years; women 43.0 ± 18.1 years, 24 to 73 years, see Table 1) participated in this study. All individuals were right-handed according to the Edinburgh inventory (Oldfield, 1971). Conventional MR images of all subjects were acquired to exclude brain morphometric abnormalities. Subjects with neurological illness, head trauma, loss of consciousness, or psychiatric disorder were also excluded. This study was approved by the Ethics and Radiation Safety Committees of the National Institute of Radiological Sciences, Chiba, Japan. All participants gave written informed consent.

DTI data acquisition and processing

Images were acquired by Philips Intera, 1.5 T (Philips Medical Systems, Best, The Netherlands). Diffusion-weighted images were acquired by single-shot echo-planar imaging with sensitivity-encoding (SENSE), parallel-imaging scheme (reduction factor = 2.0, TR = 8645 ms, TE = 96 ms). The imaging matrix was 96 × 96, with a field of view of 240 × 240 mm^2 (nominal resolution, 2.5 mm) zero-filled to 256 × 256 pixels, 60 continuous transverse slices, slice thickness 2.5 mm, b value 0 s/mm^2 (1 measurement) and 700 s/mm^2. Diffusion was measured along six non-collinear directions: $(x, y, z) = [(1, 0, 0), (0, 1, 0), (0, 0, 1), (-1/\sqrt{2}, 1/\sqrt{2}, 0), (1/\sqrt{2}, 0, -1\sqrt{2}), (0, 1/\sqrt{2}, -1/\sqrt{2})]$. The diffusion gradient pulse duration and separation were δ = 24 ms and Δ = 24 ms, respectively. Acquisition time per data set was approximately 80 s, and total scan time was 40 min. To enhance the signal-to-noise ratio, acquisition was repeated 30 times. We evaluated signal-to-noise ratio in subjects under 30 years of age (n = 13) (see Statistical analysis). The averaged images obtained with a b value of 0 s/mm^2 were used for signal-to-noise determination (Hunsche et al., 2001). Signal-to-noise ratio was defined as the quotient of the mean signal intensity in image of b value of 0 s/mm^2 and the standard deviation (SD) within centrum semiovale (Ogura et al., 2003). We did not use SD in the background noise because parallel imaging methods such as SENSE reduce the background noise level. Average signal-to-noise ratio was 22.0. This is large enough to accurately estimate parameters derived from diffusion tensor imaging, eigenvalues, and anisotropy in particular (Hunsche et al., 2001).

The DTI data sets were transferred to a workstation, and DTI quantification was preceded by eddy current correction. Each directional volume from the diffusion data set was resampled to the b = 0 image to correct for remaining eddy current distortion (Kim et al., 2002) as well as to correct for participant motion. These data realignments were performed with the use of software written in IDL Version 5.5 Win32 (×86) (Research Systems Inc., 2001). After these processes, we analyzed these data sets by using DtiStudio (H. Jiang, S. Mori; Johns Hopkins University) after all diffusion-weighted images were visually inspected for apparent artifacts due to subject motion and instrument malfunction. From b = 0 and six diffusion-weighted images, six maps of the apparent diffusion coefficient (ADC) were calculated. Solving six simultaneous equations with respect to ADC_{xx}, ADC_{xy}, etc. yielded the elements of the diffusion tensor. The diffusion tensor was then diagonalized, yielding eigenvalues $\lambda_1, \lambda_2, \lambda_3$, as well as eigenvectors that define the predominant diffusion orientation. Based on the eigenvalues, FA and MD were calculated on a voxel × voxel basis (Pierpaoli and Basser, 1996; Basser and Pierpaoli, 1998; Basser and Jones, 2002).

FA was used for the anisotropy map. The eigenvector associated with the largest eigenvalue was used as an indicator of fiber orientation. For 3D tract reconstruction, fiber assignment by means of continuous tracking, called the FACT method (Mori et al., 1999), was used. Fiber tractography was obtained with the threshold value of fiber tracking termination as FA = 0.2 and trajectory angle = 50° (Huang et al., 2005). To reconstruct tracts of interest, we used a multiple region-of-interest (ROI) approach (Mori et al., 2002). Firstly, tracking was performed from all pixels inside the brain, and results that penetrated the manually defined ROIs were assigned to the specific tracts associated with the ROIs (Wakana et al., 2004). When multiple ROIs were used for selecting tracts in the corpus callosum sub-regions, we used the CUT operation (Fig. 1) with the DtiStudio (Huang et al., 2004). ROIs for measurement of the corpus callosum sub-regions were placed using landmarks adopted previously (Witelson, 1989). The rostrum was

Table 1
Age - gender distribution of each age group

Age group	Male	Female
21 - 38 years	15	4
39 - 56 years	9	3
57 - 73 years	8	3

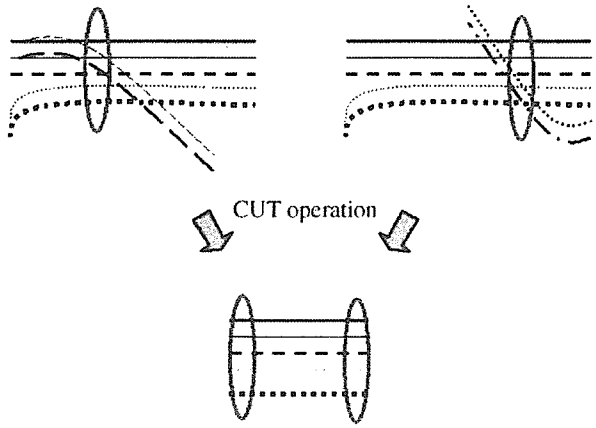

Fig. 1. CUT operation for fractional anisotropy and mean diffusivity. Diagram shows the CUT operation in this study. Two ROIs (circles) were placed on the anatomic landmarks of Fig. 2. When the CUT operation is used, tracts that run through the ROIs are selected.

treated as an extension of the genu as Witelson had pointed out in his article. In summary, six callosal subdivisions were defined as follows. The maximal length of the corpus callosum was taken as the line joining the most anterior and posterior points of the callosum. Perpendiculars to this axis were drawn at specific arithmetic divisions, resulting in six callosal segments (see Fig. 2). The ROIs of each region were plotted on the two parallel parasagittal planes located 2.8–8.4 mm (3–9 planes) on either side of the midsagittal corpus callosum. The ROIs were drawn directly onto the FA maps (Sullivan et al., 2005). The size of the fibers depended on the configuration of each region, with the fibers

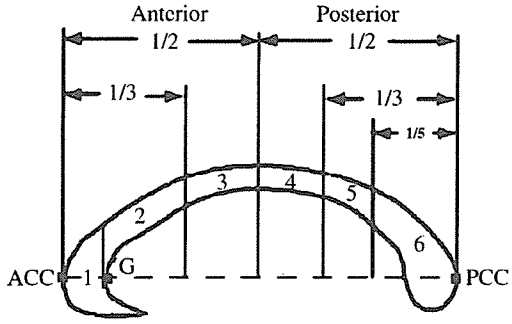

Fig. 2. Corpus callosum sub-regions. Diagram of the midsagittal view of the corpus callosum of the human adult shows the six regional subdivisions numbered 1–6. ACC and PCC indicate the anteriormost and posteriormost points of the callosum, with ACC–PCC defined as the length of the callosum. G indicates the anteriormost point on the inner convexity of the anterior callosum. ACC–PCC was used as the linear axis to subdivide the callosum into anterior and posterior halves; anterior, middle, and posterior thirds, and the posterior one-fifth region (region 6) that is roughly congruent with the splenium. The line perpendicular to the axis at point G was used to define the anteriormost division of the callosum, roughly congruent with the genu (region 1). The rostral body (region 2) was defined as the anterior one-third minus region 1. The anterior midbody (region 3) was defined as the anterior one-half minus the anterior one-third. The posterior midbody (region 4) was defined as the posterior one-half minus the posterior one-third. The isthmus (region 5) was defined as the posterior one-third minus the posterior one-fifth.

to be plotted being visually confirmed between the bilateral lateral ventricles in the $b = 0$ image. Mean FA, MD, and eigenvalues of each voxel comprising each set of fibers were measured. The object was to obtain solely white matter areas, and for the purpose of excluding visibly apparent areas of white matter hyperintensity, some fibers located on the area of white matter hyperintensity were manually excluded by NOT operation (Wakana et al., 2004). A fiber tracking example showing the parcellation of the corpus callosum of a young woman is shown in Fig. 3. Two trained operators placed the ROIs, and the reproducibilities of FA and MD values were evaluated. The coefficients of variation for these measurements were as follows: MD, 4.5%; FA, 4.7%. These were in the same range as previously reported (O'Sullivan et al., 2004).

Statistical analysis

Statistical analyses were performed with SPSS for Windows 11.0.1. j (SPSS Inc, 1989–2001). At first, sex differences for FA and MD values of the corpus callosum sub-regions were tested with analysis of variance (ANOVA) with repeated measures. Then, the relationships of the FA and MD values of the corpus callosum sub-regions with age were evaluated by Pearson's correlation method. A P value less than 0.008 (0.05/6) was considered significant to avoid type 1 errors in the multiplicity of statistical analysis. For further understanding of the environmental alterations in the aging process of the corpus callosum, the eigenvalues of the diffusion tensor were also evaluated by Pearson's correlation method (Suzuki et al., 2003; Bhagat and Beaulieu, 2004). A P value less than 0.003 (0.05/18) was considered significant.

For evaluation of the differences among the 6 divided regions of the corpus callosum, regional differences for FA values were tested with ANOVA in subjects under 30 years of age ($n = 13$) to avoid the aging effect of FA. Dunnett T3 correction was used. A P value less than 0.05 was interpreted as being statistically significant.

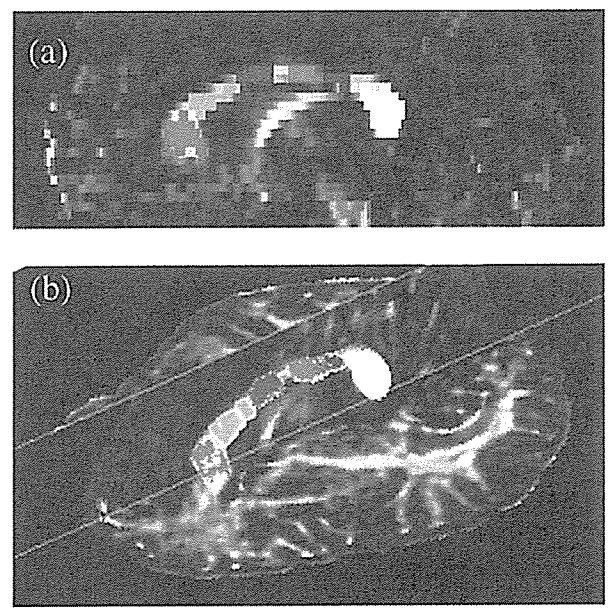

Fig. 3. Six fiber bundles projected in the corpus callosum sub-regions in midsagittal (a) and oblique from right anterior angles (b). Red, green, blue, pink, forest green, and white fibers run through the genu, rostral body, anterior midbody, posterior midbody, isthmus, and splenium, respectively.

Results

When FA in men vs. women was compared by ANOVA with repeated measures across the 6 regions, there were no significant interactions of sex × region ($F_{5200} = 1.768$; $P = 0.12$). This result corresponds well with a previous study (Hasan et al., 2005) and with the findings of a postmortem study (Aboitiz et al., 1992). MD was also compared by ANOVA with repeated measures, and there were no significant interactions of sex × region ($F_{5200} = 0.827$; $P = 0.53$). Thus, the male and female data were pooled to reduce redundant comparisons and the possible loss of statistical power due to the small populations.

The decline of FA showed a significant negative correlation with age in the genu, rostral body, and isthmus. The results are summarized in Table 2 and Fig 4. FA of the anterior midbody correlated negatively with age at a trend level ($P = 0.025$, $r = -0.35$). The increase of MD showed a significant positive correlation with age in the genu, rostral body, anterior midbody, and isthmus. The results are summarized in Table 2 and Fig. 5. The changes of eigenvalues are summarized in Table 3 and Fig 6. The increase of λ_2, λ_3, the perpendicular diffusivities, showed significant positive correlation with age in the genu, rostral body, anterior midbody, and isthmus (only λ_2 of the anterior midbody was correlated at a trend level ($P = 0.005$)). All λ_1, the parallel diffusivities, showed no correlation with age.

To assess the differences in the division of the corpus callosum into 6 regions, 13 young volunteers out of the 42 volunteers, age under 30 years (23.7 ± 1.5, mean ± SD), were evaluated for regional differences using ANOVA. ANOVA revealed that the FA values of the genu and splenium were statistically larger than those of the rostral body, anterior midbody, posterior midbody, and isthmus ($P < 0.001$, corrected). There were no differences between the genu and splenium nor between the rostral body, anterior midbody, posterior midbody and isthmus (Fig. 7).

Discussion

Previous study showed the FA values of 7 segments of the corpus callosum and the age-related change of FA in the genu and splenium (Hasan et al., 2004, 2005). In the present study, we showed the age dependence of FA, MD, and eigenvalues of the corpus callosum sub-regions with a larger number of subjects ($n = 42$). Our results showed that age is significantly correlated with FA and MD in the genu, rostral body, anterior midbody, and isthmus. FA in the genu showed a steeper decline with age than that in the splenium, a finding consistent with postmortem results (Aboitiz et al., 1996). Previous studies showed that FA declines in the genu with advancing age (Abe et al., 2000; Pfefferbaum et al., 2000; Salat et al., 2005; Sullivan et al., 2001; Hasan et al., 2004), relative anisotropy declines in the genu and splenium (Nusbaum et al., 2001), and FA declines in the genu and splenium by using fluid-attenuated inversion recovery-prepared diffusion imaging sequences (Bhagat and Beaulieu, 2004), whereas one study failed to detect age-related declines in anisotropy in the corpus callosum (Chepuri et al., 2002). However, no study had investigated the age-related decline in FA in the corpus callosum sub-regions. Using postmortem material, volume loss in the splenium with advanced age was indicated (Clarke et al., 1989), although there was no significant correlation of FA or MD with age in our study. Clarke et al. and Nusbaum et al. studied subjects more than 80 years old, while those of our study were somewhat younger. It is suggested that the splenium has subtle but increasing sensitivity to aging. Bhagat and Beaulieu showed a slight decrease in FA of the splenium compared to the genu as the FA value of older subjects (61–74 years) in the genu had reduced by 13% compared to young subjects (21–25 years) but that in the splenium decreased by only 3%. They used fluid-attenuated inversion recovery prepared diffusion imaging sequences, which allowed precise quantification of the FA values. In addition, our study showed that the observed decrease in anisotropy was due to a lack of change in λ_1 and an increase in λ_2, λ_3. It is consistent with a previous study (Bhagat and Beaulieu, 2004) and a basic pathology study that indicated a decrease in the number of myelinated nerve fibers with aging (Meier-Ruge et al., 1992).

We also showed that the mean FA values of 13 subjects in the genu and splenium were statistically larger than those in the rostral body, anterior midbody, posterior midbody, and isthmus. This result corresponds well with previous studies (Hasan et al., 2004, 2005). The trend of FA (splenium) > FA (genu) has been shown in some studies (Hasan et al., 2004, 2005; Chepuri et al., 2002; Sullivan et al., 2001). On the other hand, some studies regard FA values in the splenium and in the genu of younger subjects as almost equal (Bhagat and Beaulieu, 2004; Abe et al., 2000; Salat et al., 2005; Foong et al., 2000). Only Hasan et al. had divided the corpus callosum using landmarks adopted previously (Witelson, 1989) and showed that the FA was lower in the genu than in the splenium, but they compared FA values of subjects from 20 to 60 years old. The decrease of FA in the genu according to aging may affect the results. Some studies used a method in which the corpus callosum was subdivided into 3 regions: genu, body and splenium (Chepuri et al., 2002; Westerhausen et al., 2004). Our results showed that the FA value of the anterior one-third differs from that of the genu or rostral body. The posterior one-third also differed from the isthmus or splenium. This highlights the availability of landmarks as used in the present study for the corpus callosum subdivision (Witelson, 1989).

The sub-regions of the corpus callosum correspond to each of the specific projection areas. In this study, we found the aging

Table 2
Associations of age and FA and MD analyzed by Pearson's correlation coefficient

		Genu	RB	AMB	PMB	Isthmus	Splenium
FA	Correlation Coefficient	−0.66	−0.53	−0.35	−0.29	−0.42	−0.17
	P value	<0.001[a]	<0.001[a]	0.025[b]	0.066	0.005[a]	0.294
MD	Correlation Coefficient	0.51	0.46	0.49	0.25	0.51	0.28
	P value	0.001[a]	0.002[a]	0.001[a]	0.115	0.001[a]	0.074

RB, rostral body; AMB, anterior midbody; PMB, posterior midbody. $n = 42$.
[a] A P value less than 0.008 (0.05/6) was considered significant.
[b] Fractional anisotropy correlated negatively with age at a trend level.

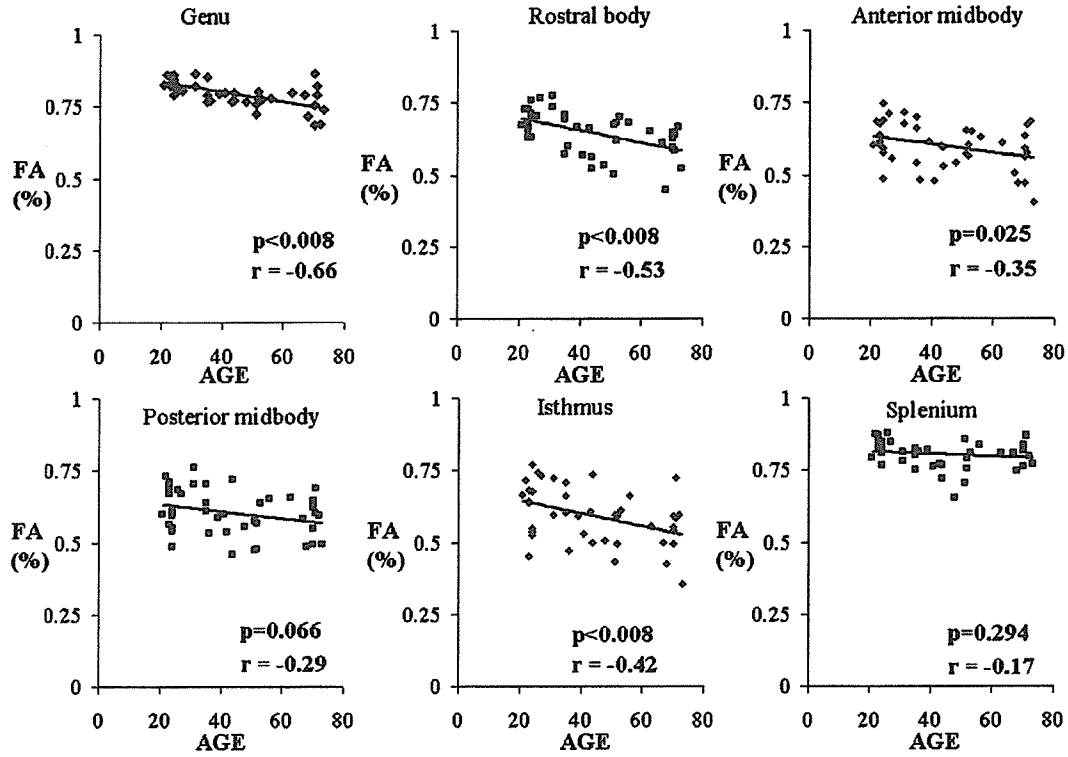

Fig. 4. FA values plotted against age. The decline of FA showed a significant negative correlation with age in the genu, rostral body, and isthmus. A P value less than 0.008 (0.05/6) was considered significant.

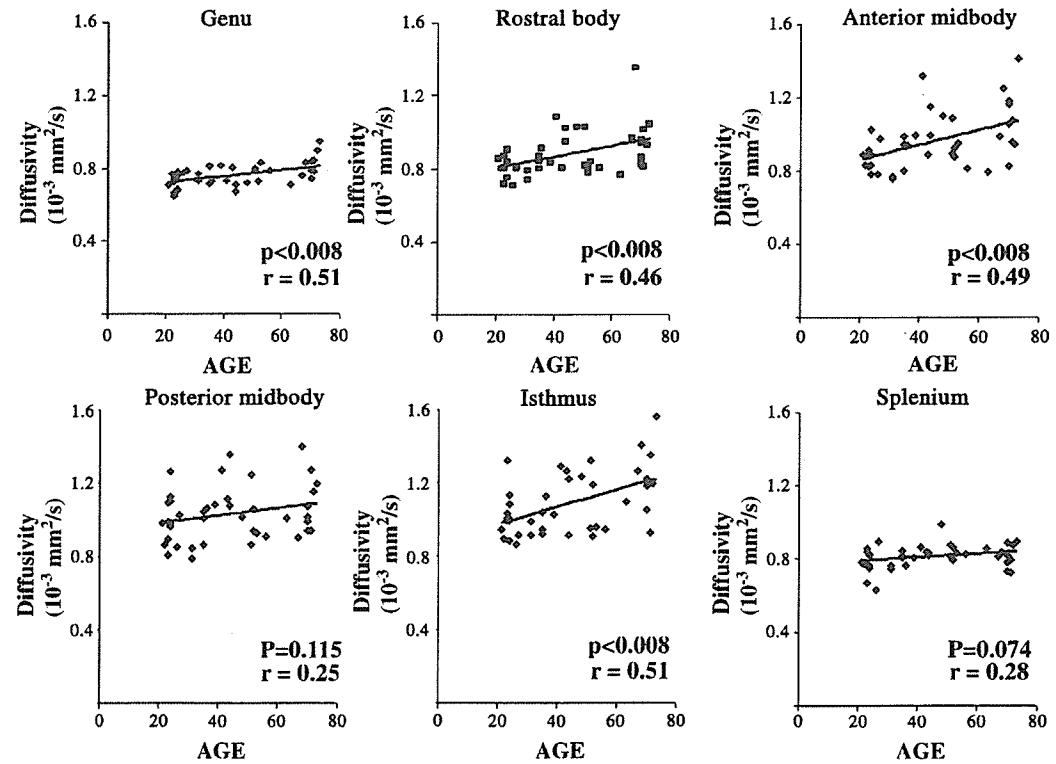

Fig. 5. MD values plotted against age. The increase of MD showed a significant positive correlation with age in the genu, rostral body, anterior midbody, and isthmus. A P value less than 0.008 (0.05/6) was considered significant.

Table 3
Associations of age and eigenvalues analyzed by Pearson's correlation coefficient

		Genu	RB	AMB	PMB	Isthmus	Splenium
λ_1	Correlation Coefficient	−0.14	0.15	0.35	0.13	0.38	0.63
	P value	0.378	0.355	0.021	0.429	0.013	0.692
λ_2	Correlation Coefficient	0.64	0.45	0.43	0.23	0.51	0.18
	P value	<0.001[a]	0.003[a]	0.005[b]	0.137	0.001[a]	0.248
λ_3	Correlation Coefficient	0.75	0.53	0.49	0.29	0.49	0.15
	P value	<0.001[a]	<0.001[a]	0.001[a]	0.068	0.001[a]	0.346

RB, rostral body; AMB, anterior midbody; PMB, posterior midbody. $n = 42$.
[a] A P value less than 0.003 (0.05/18) was considered significant.
[b] Eigenvalue correlated positively with age at a trend level.

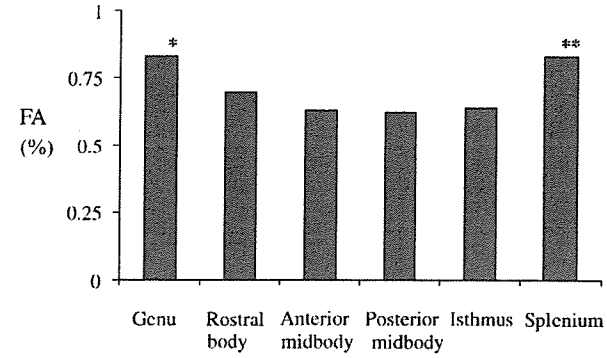

Fig. 7. Mean FA values of 13 subjects in 6 corpus callosum sub-regions. Regional differences for FA values were tested with analysis of variance (ANOVA). A P value less than 0.05 (corrected) was interpreted as being statistically significant. FA value of genu (*) was statistically larger than those of rostral body, anterior midbody, posterior midbody, and isthmus ($P < 0.001$, corrected). FA value of splenium (**) was statistically larger than those of rostral body, anterior midbody, posterior midbody, and isthmus ($P < 0.001$, corrected). There were no differences between genu and splenium nor between rostral body, anterior midbody, posterior midbody, and isthmus.

effect on FA in the genu, rostral body, and isthmus, which correspond to the frontal and parietal regions (Huang et al., 2005; Witelson, 1989) where age-related gray matter volume loss and decline in FA are observed (Good et al., 2001; Resnick et al., 2003; Sullivan et al., 2001). Relation of the corpus callosum sub-regions with disease, cognition, and development has recently been reported. The directionality of diffusion in an Alzheimer's disease group was significantly decreased in the splenium and caudal portion of the body of the corpus callosum compared with age-matched normal volunteers (Rose et al., 2000). Fibers from the splenium and caudal portion of the corpus callosum body originate from temporoparietal regions that are characteristically affected in Alzheimer's disease (Brun and Englund, 1986). In periventricular white matter injury patients with motor deficit, reduced FA was found in the body region of the corpus callosum, corresponding to the motor cortices (Thomas et al., 2005). A relation was reported between splenium FA and visual target detection task (Madden et al., 2004). Some MRI and DTI studies suggested that information on normal maturational processes from within each of the corpus callosum sub-regions could serve as markers of the developmental process across cortical regions (Innocenti, 1994; Keshavan et al., 2002; Snook et al., 2005). From these results, we suppose that fewer cortical neurons could be associated with fewer callosal fibers and that changes in FA or MD in the corpus callosum sub-

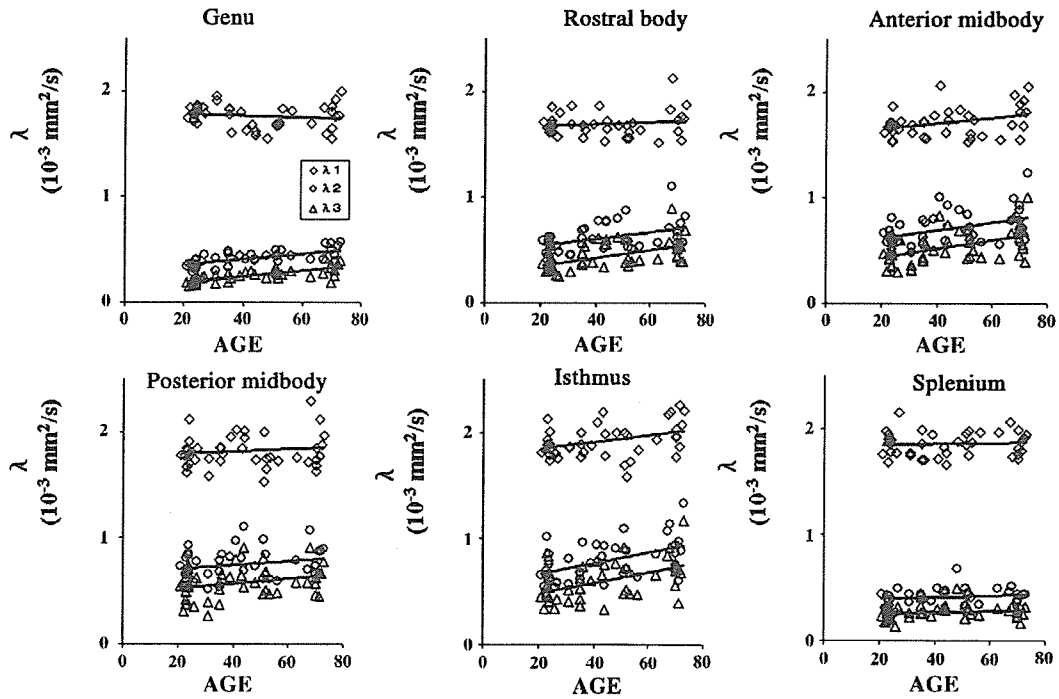

Fig. 6. Eigenvalues plotted against age. The increase of λ_2, λ_3 showed a significant positive correlation with age in the genu, rostral body, anterior midbody, and isthmus (λ_2 of the anterior midbody was at the trend level). A P value less than 0.003 (0.05/18) was considered significant.

regions may imply the degeneration of the respective projection areas. In this study, we did not detect any significant change of MD or FA in the posterior midbody or splenium nor did we find significant change of FA in the anterior midbody. These results may reflect the slight sensibility to aging of the thalamus, occipital, and temporal lobe structure (Resnick et al., 2003; Salat et al., 2005). These projection areas may obscure the aging effect on FA and MD in these sub-regions.

There is limitation to this study. In this study, the sample size of female was small. However, it has often been reported that there was no significant difference in MD or FA between males and females (Hasan et al., 2005). The smaller number of females would not be expected to make a difference. Further work with larger study populations using the same method will be necessary to confirm our results.

Correct evaluation of FA and MD in subcortical regions requires high signal-to-noise ratio, spatial resolution, and well-experienced neuroradiologists. The results of this study suggest that simple evaluation of projection areas using FA or MD in the corpus callosum sub-regions may aid in the comprehension of neurological disorders that disrupt the corresponding cortical neurons or axons.

Acknowledgments

We wish to extend our gratitude to Dr. Susumu Mori for his helpful advice and to Drs. Shoko Nozaki, Talant K. Doronbekov, and Ms. Yoshiko Fukushima for the MRI data acquisition. This research was supported by grants from the National Institute of Radiological Sciences.

References

Abe, O., Aoki, S., Hayashi, N., Yamada, H., Kunimatsu, A., Mori, H., Yoshikawa, T., Okubo, T., Ohtomo, K., 2000. Normal aging in the central nervous system: quantitative MR diffusion-tensor analysis. Neurobiol. Aging 23, 433–441.

Aboitiz, F., Scheibel, A.B., Fisher, R.S., Zaidel, E., 1992. Fiber composition of the human corpus callosum. Brain Res. 598, 143–153.

Aboitiz, F., Rodrigues, E., Olivares, R., Zaidel, E., 1996. Age-related changes in fibre composition of the human corpus callosum: sex differences. NeuroReport 7, 1761–1764.

Baird, A.A., Colvin, M.K., Vanhorn, J.D., Gazzaniga, M.S., 2005. Functional connectivity: integrating behavioral, diffusion tensor imaging, and functional magnetic resonance imaging data sets. J. Cogn. Neurosci. 17, 687–693.

Basser, P.J., Jones, D.K., 2002. Diffusion-tensor MRI: theory, experimental design and data analysis—A technical review. NMR Biomed. 15, 456–467.

Basser, P.J., Pierpaoli, C., 1996. Microstructural and physiological features of tissue elucidated by quantitative diffusion-tensor MRI. J. Magn. Reson., B 111, 209–219.

Basser, P.J., Pierpaoli, C., 1998. A simplified method to measure the diffusion tensor from seven MR images. Magn. Reson. Med. 39, 928–934.

Bhagat, Y.A., Beaulieu, C., 2004. Diffusion anisotropy in subcortical white matter and cortical gray matter: changes with aging and the role of CSF-suppression. J. Magn. Reson. Imaging 20, 216–227.

Biegon, A., Eberling, J.L., Richardson, B.C., Roos, M.S., Wong, S.T., Reed, B.R., Jagust, W.J., 1994. Human corpus callosum in aging and Alzheimer's disease: a magnetic resonance imaging study. Neurobiol. Aging 15, 393–397.

Brun, A., Englund, E., 1986. A white matter disorder in dementia of the Alzheimer type. A pathoanatomical study. Ann. Neurol. 19, 253–262.

Chepuri, N.B., Yen, Y.F., Burdette, J.H., Li, H., Moody, D.M., Maldjian, J.A., 2002. Diffusion anisotropy in the corpus callosum. Am. J. Neuroradiol. 23, 803–808.

Clarke, S., Kraftsik, R., Van der Loos, H., Innocenti, G.M., 1989. Forms and measures of adult and developing human corpus callosum: is there sexual dimorphism? J. Comp. Neurol. 280, 213–230.

Colvin, M.K., Funnell, M.G., Gazzaniga, M.S., 2005. Numerical processing in the two hemispheres: studies of a split-brain patient. Brain Cogn. 57, 43–52.

de Lacoste, M.C., Kirkpatrick, J.B., Ross, E.D., 1985. Topography of the human corpus callosum. J. Neuropathol. Exp. Neurol. 44, 578–591.

Driesen, N.R., Raz, N., 1995. The influence of sex, age, and handedness on corpus callosum morphology: a meta-analysis. Psychobiology 23, 240–247.

Duara, R., Kushch, A., Gross-Glenn, K., Barker, W.W., Jallad, B., Pascal, S., Loewenstein, D.A., Sheldon, J., Rabin, M., Levin, B., 1991. Neuroanatomic differences between dyslexic and normal readers on magnetic resonance imaging scans. Arch. Neurol. 48, 410–416.

Foong, J., Maier, M., Clark, C.A., Barker, G.J., Miller, D.H., Ron, M.A., 2000. Neuropathological abnormalities of the corpus callosum in schizophrenia: a diffusion tensor imaging study. J. Neurol. Neurosurg. Psychiatry 68, 242–244.

Good, C.D., Johnsrude, I., Ashburner, J., Henson, R.N.A., Friston, K.J., Frackowiak, R.S.J., 2001. Cerebral asymmetry and the effect of sex and handedness on brain structure: a voxel-based morphometric analysis of 465 normal adult human brains. NeuroImage 14, 685–700.

Hasan, K.M., Kanabar, B.P., Santos, R.M., Ewing-Cobbs, L., Narayana, P.A., 2004. Age dependence of the fractional anisotropy of genu and splenium of human corpus callosum using optimized DT-MRI. Proc. 12th International Society of Magnetic Resonance in Medicine, Kyoto, Japan, pp. 338.

Hasan, K.M., Gupta, R.K., Santos, R.M., Wolinsky, J.S., Narayana, P.A., 2005. Diffusion tensor fractional anisotropy of the normal-appearing seven segments of the corpus callosum in healthy adults and relapsing–remitting multiple sclerosis patients. J. Magn. Reson. Imaging 21, 735–743.

Huang, H., Zhang, J., van Zijl, P.C.M., Mori, S., 2004. Analysis of noise effects on DTI-based tractography using the brute-force and multi-ROI approach. Magn. Reson. Med. 52, 559–565.

Huang, H., Zhang, J., Jiang, H., Wakana, S., Poetscher, L., Miller, M.I., van Zijl, P.C.M., Hillis, A.E., Wytik, R., Mori, S., 2005. DTI tractography based parcellation of white matter: application of the mid-sagittal morphology of corpus callosum. NeuroImage 26, 295–305.

Hunsche, S., Moseley, M.E., Stoeter, P., Hedehus, M., 2001. Diffusion-tensor MR imaging at 1.5 and 3.0 T: initial observations. Radiology 221, 550–556.

Innocenti, G.M., 1994. Some new trends in the study of the corpus callosum. Behav. Brain Res. 64, 1–8.

Kantarci, K., Jack Jr., C.R., Xu, Y.C., Campeau, N.G., O'Brien, P.C., Smith, G.E., Ivnik, R.J., Boeve, B.F., Kokmen, E., Tangalos, E.G., Petersen, R.C., 2001. Mild cognitive impairment and Alzheimer disease: regional diffusivity of water. Radiology 219, 101–107.

Keshavan, M.S., Diwadkar, V.A., Bagwell, W.W., Harenski, K., Rosenberg, D.R., Sweeney, J.A., Haas, G.L., Pettegrew, J.W., 2002. Abnormalities of the corpus callosum in first-episode treatment-naive schizophrenia. J. Neurol. Neurosurg. Psychiatry 72, 757–760.

Kim, J.S., Kanaan, R.A., Pearlson, G.P., 2002. Extended mutual information registration for simultaneously correcting motion effects and eddy current distortion of single-shot echo-planar diffusion tensor imaging. The Eighth International Conference on Functional Mapping of the Human Brain, Sendai, Japan.

Le Bihan, D., 1995. Molecular diffusion, tissue microdynamics and microstructure. NMR Biomed. 8, 375–386.

Le Bihan, D., 2003. Looking into the functional architecture of the brain with diffusion MRI. Nat. Rev., Neurosci. 4, 469–480.

Madden, D.J., Whiting, W.L., Huettel, S.A., White, L.E., MacFall, J.R., Provenzale, J.M., 2004. Diffusion tensor imaging of adult age differences in cerebral white matter: relation to response time. NeuroImage 21, 1174–1181.

Mazziotta, J., Toga, A., Evans, A., Fox, P., Lancaster, J., Zilles, K., Woods, R., Paus, T., Simpson, G., Pike, B., Holmes, C., Collins, L., Thompson, P., MacDonald, D., Iacoboni, M., Schormann, T., Amunts, K., Palomero-Gallagher, N., Geyer, S., Parsons, L., Narr, K., Kabani, N., Le Goualher, G., Feidler, J., Smith, K., Boomsma, D., Hulshoff Pol, H., Cannon, T., Kawashima, R., Mazoyer, B., 2001. A four-dimensional probabilistic atlas of the human brain. Am. Med. Inform. Assoc. 8, 401–430.

Meier-Ruge, W., Ulrich, J., Bruhlmann, M., Meier, E., 1992. Age-related white matter atrophy in the human brain. Ann. N. Y. Acad. Sci. 673, 260–269.

Mori, S., Crain, B.J., Chacko, V.P., van Zijl, P.C., 1999. Three-dimensional tracking of axonal projections in the brain by magnetic resonance imaging. Ann. Neurol. 45, 265–269.

Mori, S., Kaufmann, W.E., Davatzikos, C., Stieltjes, B., Amodei, L., Fredericksen, K., Pearlson, G.D., Melhem, E.R., Solaiyappan, M., Raymond, G.V., Moser, H.W., van Zijl, P.C., 2002. Imaging cortical association tracts in the human brain using diffusion-tensor-based axonal tracking. Magn. Reson. Med. 47, 215–223.

Nusbaum, A.O., Tang, C.Y., Buchsbaum, M.S., Wei, T.C., Atlas, S.W., 2001. Regional and global changes in cerebral diffusion with normal aging. Am. J. Neuroradiol. 22, 136–142.

Ogura, A., Miyai, A., Maeda, F., Fukutake, H., Kikumoto, R., 2003. Accuracy of signal-to-noise ratio measurement method for magnetic resonance images. Nippon Hoshasen Gijutsu Gakkai Zasshi 59, 508–513.

Oldfield, R.C., 1971. The assessment and analysis of handedness: the Edinburgh inventory. Neuropsychologia 9, 97–113.

O'Sullivan, M., Singhal, S., Charlton, R., Markus, H.S., 2004. Diffusion tensor imaging of thalamus correlates with cognition in CADASIL without dementia. Neurology 62, 702–707.

Pfefferbaum, A., Lim, K.O., Desmond, J., Sullivan, E.V., 1996. Thinning of the corpus callosum in older alcoholic men: a magnetic resonance imaging study. Alcohol., Clin. Exp. Res. 20, 752–757.

Pfefferbaum, A., Sullivan, E.V., Hedehus, M., Lim, K.O., Adalsteinsson, E., Moseley, M., 2000. Age-related decline in brain white matter anisotropy measured with spatially corrected echo-planar diffusion tensor imaging. Magn. Reson. Med. 44, 259–268.

Pierpaoli, C., Basser, P.J., 1996. Toward a quantitative assessment of diffusion anisotropy. Magn. Res. Med. 36, 893–906 (Erratum in: Magn Reson Med 1997, 37, 972).

Resnick, S.M., Pham, D.L., Kraut, M.A., Zonderman, A.B., Davatzikos, C., 2003. Longitudinal magnetic resonance imaging studies of older adults: a shrinking brain. J. Neurosci. 23, 3295–3301.

Rose, S.E., Chen, F., Chalk, J.B., Zelaya, F.O., Strugnell, W.E., Benson, M., Semple, J., Doddrell, D.M., 2000. Loss of connectivity in Alzheimer's disease: an evaluation of white matter tract integrity with colour coded MR diffusion tensor imaging. J. Neurol. Neurosurg. Psychiatry 69, 528–530.

Salat, D., Ward, A., Kaye, J.A., Janowsky, J.S., 1997. Sex differences in the corpus callosum with aging. Neurobiol. Aging 18, 191–197.

Salat, D.H., Tuch, D.S., Greve, D.N., van der Kouwe, A.J.W., Hevelone, N.D., Zaleta, A.K., Rosen, B.R., Fischl, B., Corkin, S., Rosas, H.D., Dale, A.M., 2005. Age-related alteration in white matter microstructure measured by diffusion tensor imaging. Neurobiol. Aging 26, 1215–1227.

Schwartz, M.L., Goldman-Rakic, P.S., 1991. Prenatal specification of callosal connections in rhesus monkey. J. Comp. Neurol. 307, 144–162.

Seltzer, B., Pandya, D.N., 1986. Posterior parietal projections to the intraparietal sulcus of the rhesus monkey. Exp. Brain Res. 62, 459–469.

Snook, L., Paulson, L.A., Roy, D., Phillips, L., Beaulieu, C., 2005. Diffusion tensor imaging of neurodevelopment in children and young adults. NeuroImage 26, 1164–1173.

Sullivan, E.V., Adalsteinsson, E., Hedehus, M., Ju, C., Moseley, M., Lim, K.O., Pfefferbaum, A., 2001. Equivalent disruption of regional white matter microstructure in aging healthy men and women. NeuroReport 12, 99–104.

Sullivan, E.V., Adalsteinsson, E., Pfefferbaum, A., 2005. Selective age-related degradation of anterior callosal fiber bundles quantified in vivo with fiber tracking. Cereb. Cortex (Advanced access published on October 5, 2005; doi:10.1093/cercor/bhj045).

Suzuki, Y., Matsuzawa, H., Kwee, I.L., Nakada, T., 2003. Absolute eigenvalue diffusion tensor analysis for human brain maturation. NMR Biomed. 16, 257–260.

Thomas, B., Eyssen, M., Peeters, R., Molenaers, G., van Hecke, P., de Cock, P., Sunaert, S., 2005. Quantitative diffusion tensor imaging in cerebral palsy due to periventricular white matter injury. Brain 128, 2562–2577.

Wakana, S., Jiang, H., Nagae-Poetscher, L.M., van Zijl, P.C.M., Mori, S., 2004. Fiber tract-based atlas of human white matter anatomy. Radiology 230, 77–87.

Westerhausen, R., Kreuder, F., Dos Santos Sequeira, S., Walter, C., Woerner, W., Wittling, R.A., Schweiger, E., Wittling, W., 2004. Effects of handedness and gender on macro- and microstructure of the corpus callosum and its subregions: a combined high-resolution and diffusion-tensor MRI study. Brain Res. Cogn. Brain Res. 21, 418–426.

Witelson, S.F., 1989. Hand and sex differences in the isthmus and genu of the human corpus callosum. Brain 112, 799–835.

Yazgan, M.Y., Kinsbourne, M., 2003. Functional consequences of changes in callosal area in Tourette's syndrome and attention deficit/hyperactivity disorder. In: Zaidel, E., Iacoboni, M. (Eds.), The Parallel Brain: The Cognitive Neuroscience of the Corpus Callosum. The MIT Press, Cambridge, pp. 423–432.

International Journal of Neuropsychopharmacology (2007), 10, 281–283. Copyright © 2006 CINP
doi:10.1017/S1461145706007000

BRIEF REPORT

CINP

A preliminary open-label study of 5-HT_{1A} partial agonist tandospirone for behavioural and psychological symptoms associated with dementia

Shinji Sato[1], Katsuyoshi Mizukami[2] and Takashi Asada[2]

[1] *Department of Psychiatry, Tsukuba Memorial Hospital, Tsukuba, Japan*
[2] *Department of Neuropsychiatry, Institute of Clinical Medicine, Tsukuba University, Tsukuba, Japan*

Abstract

The aim of this study was to assess the efficacy and safety of tandospirone, a 5-HT_{1A} partial agonist, for treatment of behavioural and psychological symptoms of dementia (BPSD). Thirteen outpatients with DSM-IV diagnosis of Alzheimer's type or vascular dementia were enrolled in this study. Their BPSD and cognitive functions were evaluated with the Neuropsychiatric Inventory (NPI) and Mini-Mental State Examination, respectively, for an 8-wk period of treatment. The maximum benefit of tandospirone was achieved at a mean dose of 19.6 mg/d. There were significant improvements in the NPI subscores for delusion, agitation, depression, anxiety, and irritability at 2 or 4 wk after the start of administration of tandospirone. No patients experienced severe adverse effects. The results suggest that tandospirone was effective at improving BPSD symptoms and well-tolerated in elderly demented patients.

Received 23 March 2006; Reviewed 11 April 2006; Revised 9 May 2006; Accepted 13 May 2006; First published online 3 July 2006

Key words: Behavioural and psychological symptoms of dementia, dementia, tandospirone, 5-HT_{1A} agonist.

Introduction

The International Psychiatric Association defines Behavioral and Psychological Symptoms of Dementia (BPSD) as non-cognitive symptoms such as behaviour (e.g. agitation, aggression, wandering, screaming) and psychiatric disturbances (e.g. hallucination, delusion, depression, anxiety, insomnia). In a previous study, BPSD was observed in 20–80% of patients with dementia (Lawlor, 2004). BPSD often could have a negative impact on patients' daily activities, and especially on caregivers' quality of life (Lawlor, 2004). Although non- pharmacological interventions should be a first-line treatment for BPSD, severe BPSD often needs to be managed with psychotropic agents, especially atypical neuroleptics such as risperidone, olanzapine, and quetiapine (Lawlor, 2004). Recently, increased mortality has been reported in elderly patients with dementia using atypical antipsychotics (Food and Drug Administration, 2005) as well as conventional antipsychotic medications (Wang et al., 2005). Thus, it is crucial to develop a safer treatment for BPSD in demented patients.

Tandospirone citrate, a 5-HT_{1A} partial agonist produced in Japan, is an anxiolytic azapirone, and has shown anti-anxiety effects as well as antidepressant effects with remarkable tolerability (Murasaki et al., 1992). Although there have been only a few reports regarding the effects of tandospirone on BPSD, buspirone, a 5-HT_{1A} partial agonist like tandospirone, has been reported to be effective at managing agitation or aggressive behaviour, and to be well tolerated in patients with dementia (Cantillon et al., 1996). Here, we report the usefulness of tandospirone for treating various behavioural and psychological symptoms of dementia.

Method

Subjects

Thirteen subjects were recruited from the outpatient clinic of Tsukuba Central Hospital between April 2003 and April 2004. All had either Alzheimer's disease

Address for correspondence: K. Mizukami, M.D., Ph.D., Department of Psychiatry, Institute of Clinical Medicine, University of Tsukuba, 1-1-1 Tennodai, Tsukuba, Ibaraki 305-8575, Japan.
Tel.: (+81)29-853-3210 *Fax*: (+81)29-853-3182
E-mail: mizukami@md.tsukuba.ac.jp

Table 1. Mean (S.D.) of Neuropsychiatric Inventory (NPI) scores at each time-point with tandospirone ($n=13$)

Subscale	Baseline	2 wk after	4 wk after	6 wk after	8 wk after
Delusion	5.2 (4.9)	3.9 (3.8)	3.1 (3.0)*	3.5 (2.8)	3.5 (2.8)
Hallucination	0.9 (3.3)	0.9 (3.3)	0.1 (0.3)	0.7 (2.2)	0.7 (2.2)
Agitation/Aggression	6.6 (4.4)	4.5 (3.5)*	3.4 (2.6)**	3.2 (2.5)**	3.2 (2.5)**
Depression/Dysphoria	4.2 (5.3)	3.4 (4.1)	2.2 (2.7)*	2.2 (2.8)*	2.0 (2.7)*
Anxiety	5.8 (5.2)	4.2 (3.9)*	3.2 (2.8)*	2.9 (2.6)*	2.5 (2.0)*
Euphoria/Elation	0.0 (0.0)	0.0 (0.0)	0.0 (0.0)	0.0 (0.0)	0.0 (0.0)
Apathy/Indifference	4.9 (4.1)	4.6 (3.9)	4.6 (3.9)	4.6 (3.9)	4.6 (3.9)
Disinhibition	1.5 (2.7)	1.5 (2.7)	0.8 (1.3)	0.8 (1.3)	0.9 (1.4)
Irritability/Lability	6.5 (4.5)	4.4 (4.0)*	2.7 (2.8)**	2.6 (2.9)**	2.6 (2.9)**
Aberrant motor behaviour	5.2 (4.6)	4.8 (4.6)	3.9 (4.4)	3.9 (4.4)	3.9 (4.4)

NPI subscale scores at each time-point were compared to baseline scores using the Wilcoxon signed-rank test.
* $p<0.05$, ** $p<0.01$.

(AD) or vascular dementia (VD), according to DSM-IV (APA, 1994) diagnostic criteria, and exhibited one or more BPSD symptoms that had been unmanageable with non-pharmacotherapy for at least 1 month. All patients and their caregivers provided written informed consent for study participation; if a patient lacked the ability to give consent, we obtained it from his/her caregiver. The patients underwent physical, neurological, and laboratory examinations as well as brain magnetic resonance imaging or brain computed tomography. If they had a serious physical illness or a past history of mental or neurological disorders, they were excluded from the study.

Study design

The trial was an open-label, 8-wk study. The Mini-Mental State Examination (MMSE) and Clinical Global Impression (CGI) Rating Scale were used to assess the severity of cognitive deficits at baseline, and to evaluate the clinical improvements at 8 wk. The frequency and severity of BPSD were assessed according to the Neuropsychiatric Inventory (NPI; Cummings et al., 1994) at baseline and 2, 4, 6, and 8 wk after the start of tandospirone administration. Initially, the administration of tandospirone started at 10 mg/d, divided into morning and evening doses. If the efficacy was deemed insufficient, the daily dose was increased weekly by 5 mg/d to a maximum dose of 30 mg/d. The maximum effective and tolerated dose was determined based on clinical judgment and NPI scores. Ten patients in this study were receiving other medications (tiapride 3, donepezil 4, risperidone 2, and mianserine 2) at the study's start. These medications were continued at the same dose. We did not add or change any psychotropic medications during the investigation. Changes in the NPI scores were analysed by means of the Wilcoxon signed-rank test.

Results

All patients completed this trial. Their mean age was 76.7 ± 7.8 (range 67–93) yr, and seven (53.8%) of the 13 patients were male. Among the patients analysed, six (46.2%) had AD and seven (53.8%) had VD. Their baseline MMSE score was 13.9 ± 6.5 (range 0–22). The maximum benefit of tandospirone was achieved at 19.6 ± 8.0 mg/d (range 10–30). No serious adverse effects were observed during the study. The efficacy evaluations at each time-point are shown in Table 1. At 8 wk, scores for agitation/aggression, anxiety, irritability/lability, and depression/dysphoria significantly improved. These symptoms, except for depression/dysphoria, had already improved at 2 wk after the treatment with tandospirone, while the depression/dysphoria score significantly improved 4 wk after the treatments start. For evaluation of CGI, clinical improvements of the BPSD were observed in 10 (77%) of the 13 patients (6 very much improved, 1 much improved, 3 minimally improved, 2 no change, 1 minimally worse).

Despite study design limitation, this open-label pilot trial suggests that moderate doses of tandospirone (mean dose 19.6 mg/d) significantly reduced the severity and frequency of BPSD, including psychological symptoms such as depression, anxiety, and irritability/lability, as well as behavioural symptoms such as agitation and aggression. In addition, approximately 70% of the subjects showed clinical improvements in the symptoms evaluated by CGI. No patients showed serious adverse effects such as extrapyramidal symptoms and drowsiness, which

are often observed in patients taking neuroleptics and benzodiazepine. Collectively, our study suggests that tandospirone is an effective and well-tolerated treatment for BPSD.

Discussion

Recently, the effects of busipirone, a 5-HT_{1A} partial agonist like tandospirone, on aggression and agitation in demented patients have been reported (Cantillon et al., 1996). Lai et al. (2003) have reported that the 5-HT_{1A} receptor density in brains of AD patients correlates negatively with the maladaptive behaviour of aggression. It has also been reported that in a case study, tandospirone improved aggression in four out of seven demented patients (Yamane, 2001). The present study suggests that tandospirone is effective for aggression and agitation in patients with dementia, presumably due to improvements in serotonergic dysfunction in the brain. We also observed the effects of tandospirone on depression and anxiety symptoms of patients with dementia in this study. A double-blind study comparing tandospirone and diazepam for the treatment of neurosis demonstrated that tandospirone has shown anti-anxiety effects similar to diazepam, and also that tandospirone had anti-depressant effects (Murasaki et al., 1992). In a prior study of nine demented patients with depressive symptoms, 15 mg/d tandospirone manifested an effect on depressive symptoms (Masuda et al., 2002). The results of our study are consistent with those of these prior studies. In addition, our study showed improvements in agitation/aggression, anxiety, and irritability/lability at 2 wk, thus indicating that tandospirone takes effect relatively soon after commencing treatment. Recently, Sumiyoshi et al. (2001) reported that tandospirone is useful for improving cognitive performance in patients with schizophrenia. Although it remains to be determined if tandospirone improves cognitive function in patients with dementia, it is reasonable to suppose that tandospirone is also safe with respect to cognitive function, since neuroleptics often induce aggravation of cognitive function in patients with dementia.

In the present study, tandospirone showed a lack of severe adverse effects, and was effective for various BPSD; thus, tandospirone is a promising medicine for safely managing BPSD.

Acknowledgements

None.

Statement of Interest

None.

References

APA (1994). *Diagnostic and Statistical Manual of Mental Disorders* (4th edn). Washington, DC: American Psychiatric Association.

Cantillon M, Brunswick R, Molina D, Bahro M (1996). Buspirone vs. haloperidol: a double-blind trial for agitation in a nursing home population with Alzheimer's disease. *American Journal of Geriatric Psychiatry 4*, 263–267.

Cummings JL, Mega M, Gray K, Rosenberg-Thompson S, Carusi DA, Gornbein J (1994). The Neuropsyhciatric Inventory: comprehensive assessment of psychopathology in dementia. *Neurology 44*, 2308–2314.

Food and Drug Administration (2005). FDA Public Health Advisory: deaths with Antipsychotics in Elderly Patients with Behavioral Disturbances, 11 April 2005. (http//www.fda.gov/cder/drug/advisory/antipsychotic.htm). Accessed 21 July 2005.

Lai MK, Tsang SW, Francis PT, Esiri MM, Keene J, Hope T (2003). Reduced serotonin 5-HT1A receptor binding in the temporal cortex correlates with aggressive behavior in Alzheimer's disease. *Brain Research 974*, 82–87.

Lawlor BA (2004). Behavioral and psychological symptoms in dementia: the role of atypical antipsychotics. *Journal of Clinical Psychiatry 65* (Suppl. 11), 5–10.

Masuda Y, Akagawa Y, Hishikawa Y (2002). Effect of serotonin 1A agonist tandospirone on depression symptoms in senile patients with dementia. *Human Psychopharmacology: Clinical and Experimental 17*, 191–193.

Murasaki M, Mori A, Endo S, Takemasa K, Hasegawa K, Kamishima K (1992). Efficacy of a new anxiolytic, tandospirone (SM-3997) on neurosis [in Japanese]. *Clinical Evaluation 20*, 295–329.

Sumiyoshi T, Matsui M, Nohara S, Yamashita I, Kurachi M, Sumiyoshi C, Jayathilake K, Meltzer HY (2001). Enhancement of cognitive performance in schizophrenia by addition of tandospirone to neuroleptic treatment. *American Journal of Psychiatry 158*, 1722–1725.

Wang PS, Schneeweiss S, Avorn J, Fischer MA, Mogun H, Solomon DH (2005). Risk of death in elderly users of conventional vs. atypical antipsychotic medications. *New England Journal of Medicine 353*, 2335–2341.

Yamane H (2001). Tandospirone clinical adaptation of dementia with aggression [in Japanese]. *Japanese Journal of Psychiatric Treatment 16*, 169–172.

Available online at www.sciencedirect.com

ScienceDirect

Neuroscience Letters 407 (2006) 234–239

Neuroscience Letters

www.elsevier.com/locate/neulet

Relationship between diffusion tensor imaging and brain morphology in patients with myotonic dystrophy

Miho Ota[a], Noriko Sato[a,*], Yasushi Ohya[c], Yoshitsugu Aoki[c], Katsuyoshi Mizukami[b], Takeyuki Mori[a], Takashi Asada[b]

[a] *Department of Radiology, National Center Hospital for Mental, Nervous and Muscular Disorders, National Center of Neurology and Psychiatry, 4-1-1 Ogawahigashi, Kodaira, Tokyo 187-8551, Japan*

[b] *Department of Neuropsychiatry, Institute of Clinical Medicine, University of Tsukuba, 1-1-1 Tennoudai, Tsukuba, Ibaraki 305-8575, Japan*

[c] *Department of Neurology, National Center Hospital for Mental, Nervous and Muscular Disorders, National Center of Neurology and Psychiatry, 4-1-1 Ogawahigashi, Kodaira, Tokyo 187-8551, Japan*

Received 14 July 2006; received in revised form 21 August 2006; accepted 29 August 2006

Abstract

Myotonic dystrophy type 1 (MyD) is a common inherited neuromuscular disorder. In addition to neuromuscular symptoms, many MyD patients show central nervous system neuropathology. This study evaluated whether MyD patients display diffusion tensor (DT) abnormalities associated with regional cortical atrophy and clinical features. Three-dimensional T1-weighted and DT magnetic resonance images of the brain were obtained in 11 MyD patients and 13 age- and sex-matched healthy subjects. Fractional anisotropy (FA) and mean diffusivity (MD) values were calculated in corpus callosum subregions with DT imaging (DTI) along with volumetric changes, and correlations with clinical features were examined. Differences between MyD patients and healthy subjects were analyzed statistically. Significantly lower FA and higher MD values were found in the genu, rostral body, anterior midbody, posterior midbody and splenium in MyD patients than in control subjects ($p < 0.05$, corrected; lower FA in the splenium was at a trend level). These corpus callosum subregions were the areas connected to cortical areas where significantly lower volumes were found in MyD patients. No significant decrease in volumes was noted in the parietal cortex, where connecting fibers pass through the isthmus in which DTI abnormalities were not detected in MyD patients. Significant negative correlations to volumes of frontal areas were noted, particularly bilateral motor areas, with cytosine thymine guanidine (CTG) triplet expansion. DTI results in corpus callosum may reflect morphological changes in the connecting cortical areas of MyD patients.

Keywords: Myotonic dystrophy; Fractional anisotropy; Mean diffusivity; Voxel-based morphometry; CTG repeat

Myotonic dystrophy (MyD) is a hereditary disease characterized by muscular atrophy and myotonia associated with various systematic abnormalities, including some in the central nervous system [11]. MyD patients display cognitive disorder, personality change and hypersomnia. This progressive autosomal dominant, multisystemic disease is characterized by an unstable triplet cytosine thymine guanidine (CTG) repeat on chromosome 19, which appears to be excessively amplified [8].

Previous magnetic resonance imaging (MRI) studies of the brain have shown ventriculomegaly, scattered patches of increased signal in white matter, and cortical atrophy in MyD patients [1,4]. Some pathological data concerning brain involvement in MyD have shown central nervous system neuropathology, cell loss in the cerebral cortex, neuronal inclusion bodies mostly in the thalamus, caudate and other brainstem nuclei, decreased myelin sheathing, and increased neurofibrillary tangles [11,18]. However, few studies have examined relationships between morphometic or microstructural changes of the brain and disease severity.

Diffusion tensor imaging (DTI) is a sophisticated MRI technique that reveals tissue microstructure [16,17], allows in vivo white matter tract imaging [2], and provides measures of both diffusivity (a measure of mean diffusivity (MD), averaged in all spatial directions) and fractional anisotropy (FA), a measure of the directionality of diffusion [22]. DTI analysis of cerebral white matter in MyD patients has been reported

* Corresponding author. Tel.: +81 42 341 2711; fax: +81 42 346 2094.
E-mail address: snoriko@ncnp.go.jp (N. Sato).

0304-3940/$ – see front matter © 2006 Elsevier Ireland Ltd. All rights reserved.
doi:10.1016/j.neulet.2006.08.077

previously [9,23], but scattered patches of increased signal in white matter made microstructural changes in manually plotted regions of interest (ROIs) difficult to discuss.

The corpus callosum (CC) displays heterotopic anteroposterior cortical connectivity. Furthermore, specific regions of the CC (i.e., genu, rostral body, anterior midbody, posterior midbody, isthmus and splenium) comprise fibers connecting hetero- and unimodally associated cortical regions [13,25]. The genu, rostral body, anterior midbody, posterior midbody, isthmus and splenium comprise fibers connecting caudal/orbital prefrontal areas and inferior premotor area, prefrontal area, frontal area and motor system, frontal area and motor system, parietal area, temporal and occipital areas, respectively, and the FA and MD values of CC subregions are linked to the associated regions [12,21]. Evaluation of normal-appearing white matter of the CC subregions could be used as a marker of the projection area, where ROIs are difficult to place.

This study performed DTI and voxel-based morphometry (VBM), which can be used to evaluate regional changes in brain volumes, to determine whether MyD patients have DT abnormalities associated with regional cortical atrophy. Furthermore, we also evaluated relationships between these MR data and various clinical features, such as CTG triplet expansion.

A total of 11 MyD patients (six men, five women; mean age, 56.6 ± 8.6 years; mean duration of illness 28.5 ± 15.5 years; mean age at onset, 28.2 ± 13.8 years) and 13 sex- and age-matched healthy subjects (six men, seven women; mean age, 56.3 ± 12.5 years) were examined. Patients with congenital MyD or any other neurological disease, and healthy subjects with neurological illness, head trauma, loss of consciousness or psychiatric disorder were excluded. Diagnosis was made based on family history, presence of myotonia on clinical examination and/or myotonic discharge on electromyographic examination. Diagnosis was confirmed by linkage analysis using DNA markers on chromosome 19 evaluated in all patients from leukocytes and showing abnormally numerous repeats of the CTG fragment. For clinical data, disease duration, age at onset and age at scan date were examined, in addition to repeats of CTG triplet expansion in each patient. All participants provided written informed consent, and the protocol was approved by the local ethics committee.

MR images were performed on a 1.0-T Magnetom Harmony system (Siemens, Erlangen, Germany). DTI was performed in the axial plane (echo time (TE)/repetition time (TR), 113/10,100 ms; field of view (FOV), 230 mm × 230 mm; matrix, 128 × 128; 40 continuous transverse slices; slice thickness 3 mm with no interslice gap). To enhance the signal-to-noise ratio, acquisition was repeated 5 times. Diffusion was measured along 12 non-collinear directions ($(x, y, z) = [(1, 0, 0.5)\ (0, 0.5, 1)\ (0.5, 1, 0)\ (1, 0.5, 0)\ (0, 1, 0.5)\ (0.5, 0, 1)\ (1, 0, -0.5)\ (0, -0.5, 1)\ (-0.5, 1, 0)\ (1, -0.5, 0)\ (0, 1, -0.5)\ (-0.5, 0, 1)]$) with the use of a diffusion-weighted factor b in each direction for 700 s/mm^2, and one image was acquired without use of a diffusion gradient. The signal-to-noise ratio in the $b = 0$ image was roughly 30 in the central semiovale. This was large enough to accurately estimate the parameters [14]. The DTI examination took approximately 11 min. High spatial-resolution, 3-dimensional (3D) T1-weighted images of the brain were obtained for morphometric study. The 3D T1-weighted images were scanned in the sagittal plane (TE/TR, 3.93/2080 ms; flip angle, 15°; effective slice thickness, 1.23 mm; slab thickness, 177 mm; matrix, 208 × 256; FOV, 256 mm × 315 mm; acquisition, 1) yielding 144 contiguous slices through the head. In addition to DTI and 3D T1-weighted images, conventional axial T2-weighted turbo spin echo images (TE/TR, 89/6580 ms; flip angle, 180°; slice thickness, 5 mm; intersection gap, 0.4 mm; matrix, 128 × 128; FOV, 230 mm × 230 mm; acquisition, 1) and fluid attenuation inversion recovery images in an axial plane (TE/TR, 104/9100 ms; flip angle, 150°; slice thickness, 3 mm; intersection gap, 0 mm; matrix, 256 × 256; FOV, 230 mm × 230 mm; acquisition, 1) were acquired to exclude cerebral vascular disease. On conventional MRI, no abnormal findings were detected in the brain except for cerebral atrophy and cerebral white matter signal abnormalities compatible with MyD in all patients.

Raw diffusion tensor data were transferred to a workstation and DTI data sets were analyzed using DtiStudio software (H. Jiang, S. Mori; Johns Hopkins University). Diffusion tensor parameters were calculated on a pixel-by-pixel basis, then FA, MD, and finally 3D fiber tracts were calculated. Fiber tractography was performed with a threshold value of fiber-tracking termination of FA = 0.2 and a trajectory angle of 50° [13]. In this study, we selected the range-designated tract fibers as the ROIs for the evaluation of FA and MD in the same manner as previously reported [21,25]. Six callosal subdivisions were defined at the midsagittal plane, with the CC being divided into the genu, rostral body, anterior midbody, posterior midbody, isthmus and splenium, from anterior to posterior. The anterior half included the genu, rostral body and anterior midbody. The line perpendicular to the axis at the anterior point on the inner convexity of the anterior CC was used to define the anteriormost division of the CC, indicating the genu. The rostral body was defined as the anterior one-third minus the genu. The anterior midbody was defined as the anterior half minus the anterior one-third. The posterior half included the posterior midbody, isthmus and splenium. The posterior midbody was defined as the posterior half minus the posterior one-third. The isthmus was defined as the posterior one-third minus the posterior one-fifth. The posteriormost one-fifth of the CC represented the splenium. Next, tracts of interest were calculated between two parasagittal planes located 3.8 mm (two planes) on either side of the midsagittal CC. Mean FA and MD for each voxel comprising each set of fibers were measured. Statistical analyses were performed using SPSS for Windows 11.0.1J software (SPSS, Japan Co., Tokyo, Japan). Initially, differences in FA and MD values of the CC subregions between MyD patients and healthy subjects were evaluated using Student's t-test. Values of $p < 0.008$ ($= 0.05/6$) were considered statistically significant to avoid type 1 errors in the multiplicity of statistical analysis. Relationships of the FA and MD values of CC subregions with CTG expansion, age at onset, age at scan data, and disease duration were evaluated using Pearson's correlation method. Values of $p < 0.008$ ($= 0.05/6$) were considered significant.

To clarify volume differences between patients and healthy subjects, structural 3D T1-weighted MR images were ana-

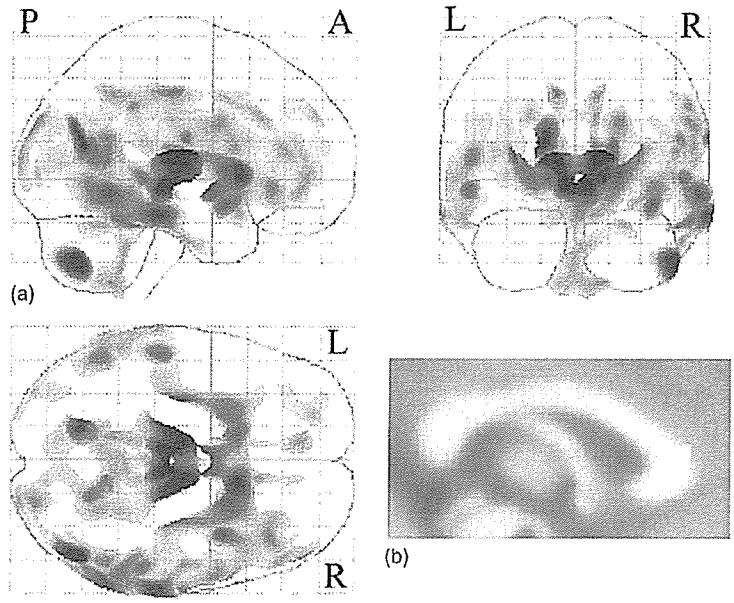

Fig. 1. (a) Regions of atrophy for gray matter in myotonic dystrophy patients compared to healthy subjects (two-sample *t*-test, SPM 2). Significant volume losses were detected in the prefrontal cortex, thalamus, striatum, temporal cortex and occipital cortex, but not in the parietal cortex. (b) Regions of atrophy for the corpus callosum in myotonic dystrophy patients compared to healthy subjects (two-sample *t*-test, SPM 2). Significant volume decrease was detected in the genu.

lyzed using an optimized VBM technique. Data were analyzed using Statistical Parametric Mapping 2 (SPM2) software (Wellcome Department of Imaging Neuroscience, London, UK) running on MATLAB 6.5 (Math Works, Natick, MA). Images were processed using optimized VBM script (dbm.neuro.uni-jena.de/vbm.html). Details of this process are described elsewhere [10]. Normalized segmented images were modulated by multiplication with Jacobian determinants of spatial normalization function to encode the deformation field for each subject as tissue density changes in normal space. Images were smoothed using a 12 mm full-width half-maximum of an isotropic Gaussian kernel. Statistical analyses were performed using SPM2 software. Differences in regional gray matter volume and white matter volume, especially callosal volume, between MyD patients and healthy subjects were assessed by the two-sample *t*-test, while the relationship between regional gray matter volume and CTG expansion, disease duration, age at onset, and age at scan date of the MyD patients was evaluated by single regression model. Only correlations that met these criteria were deemed statistically significant. In this case, a seed level of $p < 0.001$ (uncorrected) and a cluster level of $p < 0.05$ were selected.

Significant differences in FA and MD were noted between MyD patients and healthy subjects in the genu, rostral body, anterior midbody, posterior midbody and splenium (Table 1). Only the difference in FA in the splenium was at a trend level ($p = 0.019$). No significant differences were noted in the isthmus. However, no correlations were found between FA and MD values and CTG expansion, disease duration, age at onset, and age at scan date in MyD patients (data not shown).

CC subregions comprised fibers connecting associated cortical regions, so atrophy of these areas was evaluated using VBM analysis. Significantly decreased volumes in prefrontal, temporal and occipital areas, thalamus and striatum were found, but not in parietal areas (Fig. 1a), where connecting fibers pass through the isthmus. The callosal volume was also measured, with volume loss being detected only in the genu of CC subregions (Fig. 1b). Significant negative correlations were also found between cerebral volumes and CTG expansion in bilateral motor areas (Fig. 2). These areas were not correlated with disease duration, age at onset, or scan date (data not shown).

DTI was used to evaluate microstructural changes in CC subregions in 11 MyD patients. Changes in FA and MD values were detected in the genu, rostral body, anterior midbody, posterior midbody and splenium, comprising fibers connecting the frontal area, motor system, and temporal and occipital areas. No such changes were detected in the isthmus containing fibers connecting to the parietal area. Conversely, VBM analysis revealed regional volume atrophy of areas, such as the prefrontal cortex, thalamus, striatum, temporal cortex and occipital cortex, but not the parietal cortex. These changes in the microstructure of CC subregions corresponded well with atrophic cortical areas, where fibers connecting between the hemispheres ran through these CC subregions. This study also revealed that CTG expansion size correlates with volume loss of the motor and prefrontal cortices.

Only two previous studies have evaluated FA and MD changes of the brain in MyD patients, examining various white matter areas. Regarding the CC, only estimations of the genu and splenium were made, and those data were consistent with our own findings. However, no estimations of the rostral body, midbodies or isthmus were made [9,23]. Furthermore, data were obtained from manually plotted ROIs, whereas our data were obtained from 3D fiber tracts between the two parallel parasagittal planes on either side of the midsagittal CC.

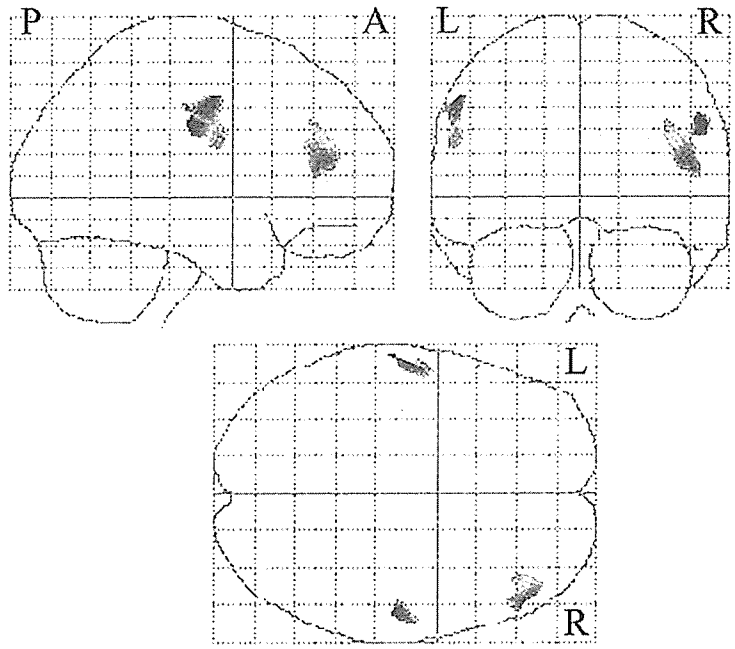

Fig. 2. Relationship between regional gray matter volume and CTG expansion in MyD patients (single regression model, SPM2). There was negative correlation between CTG expansion size and gray matter volumes of the bilateral motor area and right prefrontal cortex.

Our detailed examination showed differences in microstructural changes between the two sides.

No postmortem studies have revealed neuronal degeneration of the CC, but cortical neuronal losses are known to occur in gray matter of MyD patients [18]. These changes in CC may suggest that the loss of myelin and axonal membranes in some CC subregions may be due to Wallerian degeneration derived from atrophy of those projected cortical areas [19]. The absence of microstructural changes in the isthmus would be due to the lack of atrophic changes of the parietal cortex. The difference in FA at the splenium, which comprises fibers connecting temporal and occipital lobes, was at a trend level. In our study, regional volume losses were also revealed in temporal and occipital cortices. The failure to detect significant changes in the splenium could thus be ascribed to the degree of volume changes. In the occipital lobe, cortical atrophic changes were lower than in other cortical regions in our patients. To determine whether the changes of FA in CC subregions were related to CC subregion volume losses, we investigated the callosal volume. Significant volume decrease was shown only in the genu, not in the other CC subregions. This indicated that the reduction of callosal volume did not contribute to the reduction of anisotrophy. Furthermore, it may suggest that the microstructural changes precede the morphometrical changes of the CC subregions.

Microstructural changes in the rostral body, anterior midbody and posterior midbody would be caused not only by degeneration of the frontal area, but also by dysfunction of the motor system. Decreases in volume of the thalamus and striatum were detected in this study, and neuropathological changes in the thalamus, caudate, brainstem nuclei and the so-called motor system are well known [6,11,20]. These changes were of major interest both for research and clinical practice. However, regarding DTI analysis, the thalamus and striatum are known to display laterality and subregional differences [3,7], and comprehensive evaluation of the motor system is complicated. FA and MD values of these areas could thus serve as indices of disturbance across motor areas. The mean MD value in the isthmus of CC in normal subjects is larger than in other subregions. However, a previous study showed that the MD of the isthmus is larger and accelerated along with age compared to the other CC subregions, and the data of the present study corresponded well with the previous one [21].

In this study, correlations between DTI metrics and clinical features, such as age at scan and CTG repeat were not found. This may be due to the fact that the age distribution of MyD was quite narrow (one was 34 years old, and the others were 50–64 years old), and thus the results were not influenced by an aging effect. This VBM analysis showed a correlation between CTG repeat and the limited regional volumes. However, the FA and MD values of the CC subregions were indirect indices of the related cortical regions, and the slight changes of gray matter would not affect the FA and MD values of CC subregions.

Correlation between changes of brain structures and CTG expansion were analyzed, and it was revealed for the first time that CTG expansion size correlates with volume loss of the motor and prefrontal cortices. CTG expansion size is known to correlate with disease severity [11], cognitive executive (frontal) deficits [24], full scale intelligence quotient (IQ), performance IQ, and verbal IQ [15]. Motor areas in MyD patients were smaller than in healthy subjects [1]. Cerebral hypoperfusion of the frontal lobe and working memory deficit were also reported in MyD patients [5,15]. Our findings may explain the correlations between these changes. Previous studies were unable to detect correlations between volume and CTG expansion size

Table 1
Differences in fractional anisotropy (FA) and mean diffusivity (MD) in myotonic dystrophy (MyD) patients and healthy subjects

	Genu	RB	AMB	PMB	Isthmus	Splenium
FA in MyD patients	$0.70 \pm 0.09^{**}$ ($t = 4.56$)	$0.56 \pm 0.07^{**}$ ($t = 3.45$)	$0.60 \pm 0.10^{**}$ ($t = 3.15$)	$0.61 \pm 0.11^{**}$ ($t = 3.42$)	0.61 ± 0.08 ($t = 1.43$)	$0.77 \pm 0.07^{**}$ ($t = 2.73$)
FA in healthy subjects	0.84 ± 0.04	0.70 ± 0.12	0.72 ± 0.09	0.74 ± 0.08	0.66 ± 0.10	0.84 ± 0.04
MD in MyD patients	$10.27 \pm 1.85^{**}$ ($t = -5.13$)	$11.45 \pm 1.92^{**}$ ($t = -3.49$)	$10.82 \pm 2.79^{**}$ ($t = -2.93$)	$10.73 \pm 1.42^{**}$ ($t = -4.78$)	11.36 ± 2.06 ($t = -2.04$)	$9.00 \pm 1.10^{**}$ ($t = -4.02$)
MD in healthy subjects	7.23 ± 0.73	8.62 ± 2.06	8.38 ± 1.04	8.46 ± 0.88	9.92 ± 1.38	7.46 ± 0.78

RB: Rostral body; AMB: anterior midbody; PMB, posterior midbody; MD: (10^{-4} mm^2/s).
* Significant difference between MyD patients and healthy subjects; $p < 0.008$ ($= 0.05/6$) was considered significant.
** Difference between MyD patients and healthy subjects at a trend level ($p < 0.05$).

[11]. Participants in those studies contained patients who became ill in childhood. Patients with early onset, such as congenital MyD are known to show severe neuromuscular symptoms and CNS disorders [11]. A combination of adult and younger onset patients may thus affect the results. However, the number of patients in the present study was small, raising the question of adequate statistical power. Further studies with larger groups of patients and controls are warranted to confirm our results.

In summary, microstructural changes of FA and MD in CC subregions connecting to cortical areas correlate well with cortical volumes in MyD patients. Significant negative correlations also exist between the volume of the frontal cortex, particularly the bilateral motor areas, and CTG triplet expansion size. DTI and VBM demonstrated the presence of microstructural changes, especially in motor neurons of MyD patients.

References

[1] G. Antonini, C. Mainero, A. Romano, F. Giubilei, V. Ceschin, F. Gragnani, S. Morino, M. Fiorelli, F. Soscia, A. Di Pasquale, F. Caramia, Cerebral atrophy in myotonic dystrophy: a voxel based morphometric study, J. Neurol. Neurosurg. Psychiatry 75 (2004) 1611–1613.
[2] P.J. Basser, C. Pierpaoli, Microstructural and physiological features of tissue elucidated by quantitative diffusion-tensor MRI, J. Magn. Res. B 111 (1996) 209–219.
[3] T.E. Behrens, H. Johansen-Berg, M.W. Woolrich, S.M. Smith, C.A. Wheeler-Kingshott, P.A. Boulby, G.J. Barker, E.L. Sillery, K. Sheehan, O. Ciccarelli, A.J. Thompson, J.M. Brady, P.M. Matthews, Non-invasive mapping of connections between human thalamus and cortex using diffusion imaging, Nat. Neurosci. 6 (2003) 750–757.
[4] B. Censori, L. Provinciali, M. Danni, L. Chiaramoni, M. Maricotti, N. Foschi, M. Del Pesce, U. Salvolini, Brain involvement in myotonic dystrophy: MRI features and their relationship to clinical and cognitive conditions, Acta Neurol. Scand. 90 (1994) 211–217.
[5] L. Chang, T. Anderson, O.A. Migneco, K. Boone, C.M. Mehringer, J. Villanueva-Meyer, N. Berman, I. Mena, Cerebral abnormalities in myotonic dystrophy. Cerebral blood flow, magnetic resonance imaging, and neuropsychological tests, Arch. Neurol. 50 (1993) 917–923.
[6] A. Culebras, R.G. Feldman, F.B. Merk, Cytoplasmic inclusion bodies within neurons of the thalamus in myotonic dystrophy. A light and electron microscope study, J. Neurol. Sci. 19 (1973) 319–329.
[7] A.J. Fabiano, M.A. Horsfield, R. Bakshi, Interhemispheric asymmetry of brain diffusivity in normal individuals: a diffusion-weighted MR imaging study, Am. J. Neuroradiol. 26 (2005) 1089–1094.
[8] Y.H. Fu, A. Pizzuti, R.G. Fenwick Jr., J. King, S. Rajnarayan, P.W. Dunne, J. Dubel, G.A. Nasser, T. Ashizawa, P. DeJong, B. Wieringa, R. Korneluk, B.M. Perryman, H.F. Epstein, C.T. Caskey, An unstable triplet repeat in a gene related to myotonic dystrophy, Science 255 (1992) 1256–1258.
[9] H. Fukuda, J. Horiguchi, C. Ono, T. Ohshita, J. Takaba, K. Ito, Diffusion tensor imaging of cerebral white matter in patients with myotonic dystrophy, Acta Radiol. 46 (2005) 104–109.
[10] C.D. Good, I. Johnsrude, J. Ashburner, R.N.A. Henson, K.J. Friston, R.S.J. Frackowiak, Cerebral asymmetry and the effect of sex and handedness on brain structure: a voxel-based morphometric analysis of 465 normal adult human brains, Neuroimage 14 (2001) 685–700.
[11] P.S. Harper, Myotonic Dystrophy, Major Problems in Neurology, vol. 37, third ed., W.B. Saunders, London, 2001, pp. 139–165.
[12] K.M. Hasan, R.K. Gupta, R.M. Santos, J.S. Wolinsky, P.A. Narayana, Diffusion tensor fractional anisotropy of the normal-appearing seven segments of the corpus callosum in healthy adults and relapsing-remitting multiple sclerosis patients, J. Magn. Reson. Imag. 21 (2005) 735–743.
[13] H. Huang, J. Zhang, H. Jiang, S. Wakana, L. Poetscher, M.I. Miller, P.C.M. van Zijl, A.E. Hillis, R. Wytik, S. Mori, DTI tractography based parcellation of white matter: application of the mid-sagittal morphology of corpus callosum, Neuroimage 26 (2005) 295–305.